ELECTRONIC PROPERTIES OF FUNCTIONALIZED GNRS WITH EXTENDED HÜCKEL THEORY

A THESIS

SUBMITTED TO THE GRADUATE SCHOOL

IN PARTIAL FULFILLMENT OF THE REQUIREMENTS

FOR THE DEGREE

MASTER OF SCIENCE

BY

DUNJA MILINOVIC

ADVISOR: DR. MAHFUZA KHATUN

BALL STATE UNIVERSITY

MUNCIE, INDIANA

DECEMBER 2019

Acknowledgments

First, I would like to thank Dr. Khatun for all her effort in helping me in everything that I did. She not only took a lot of time to give me plenty of advice, but also took the time to guide me through the whole the way. I appreciate every nanosecond of her help. I would also like to thank my parents for their never-ending support, love, and kind words. They believe in me even when I do not believe in myself. They encourage me when I am stuck and push me to try harder. I am forever grateful for that.

Additionally, I would like to thank the other graduate students for their helpful conversations. It was always nice speaking to the others whether it be research related or some random physics topic or other science related discussion. I also want to thank my dear friends for cheering me on when things were rough. I appreciate every ounce of their help.

Table of Contents

List of Figures

List of Tables

Abstract

Electronic properties of graphene nanoribbons (GNRs) were investigated. Graphene nanoribbons are one-atom layer thin sheets of carbons arranged in a pattern of repeating hexagons that have a semi-infinite length and finite width. GNRs have important electronic properties, and are very useful materials in nanoelectronics and nanodevices. GNRs are either metallic or semiconducting, depending on the width of the structure and the edge structure. There are two different edge structures: armchair and zigzag. The electronic properties of these materials can be altered by functionalizing the structures. In this project, the edges of armchair graphene nanoribbons (AGNRs) were functionalized by H, N, O, F, P, S, and Cl to tune and engineer the bandgap for the application of electronic devices. A theoretical analysis via the usage of Tight-Binding Model (TB Model) with Extended Hückel Theory (EHT) and Green's Function Theory were used to calculate the electronic band structure, density of states (DOS), conductance, and local density of states (LDOS). The functionalized results are compared to the results of the perfect structure. The presence of foreign elements on the edges of graphene nanoribbons has a significant effect on the electronic properties and quantum transport.

Chapter 1: Introduction

1.1 An Overview

Nanoscience is part of the large field called Condensed Matter Physics and deals with objects that are at the nanoscale level [1-3]. This level is between 0.1 to 100 nanometers. Graphene is one atomic layer of a thin sheet of carbons arranged in a pattern of repeating hexagons [2, 4, 5]. Novoselov, *et al* were the first to isolate it back in 2004 [5-7].

Graphene is important in the field of Condensed Matter physics, and researchers are interested in its electrical properties [3, 8-17]. Graphene does not have a significant band gap, though GNRs do have a band gap due to the type of edge structure which gives unique electrical properties [18]. A strip of graphene that has finite width and semi-infinite length is called a graphene nanoribbon (GNR) [2]. GNRs are made from: the top-down approach, such as unzipping carbon nanotubes (CNTs), bottom-up synthesis, which is essentially building the material at the atomic scale, and etching methods [19].

The importance of GNRs, which are carbon allotropes, is that one can engineer band gaps of different widths for the usage in nanodevices. Several applications include the photovoltaic cells in solar panels, nanoscale transistors, capacitors, circuits, and electronic devices used in the medical, industrial, and engineering fields [3, 4, 7-9, 20]. A GNR's electronic properties are dependent on geometry [8, 21]. Bandgap engineering and the tuning of electron transport properties in GNRs are two ways to change the electrical properties [12, 19, 22]. Another way to change the electrical properties is by terminating the edges with another element [20]. Edge

effects have a big effect on the system [23]. The electronic properties depend on the size of the structure and the shape of the edges [24-26].

Graphene nanoribbons can have two different edge structures known as armchair and zigzag. It is known that two thirds of all armchair graphene nanoribbons (AGNRs) are semiconducting and that one third of all AGNRs are metallic. AGNRs are semiconducting or metallic depending on the width of the structure. All zigzag graphene nanoribbons (ZGNR) are metallic [5, 14, 27, 28]. AGNRs are described by the number of dimers, and ZGNRs are described by the number of chains [29].

In this thesis, we will explore the change of electronic properties, and several theoretical models are utilized. Tight-Binding Model (TB Model) with Hückel Theory (HT) are used in order to find the band structure and density of states (DOS). The band structure and DOS provide a lot of information on the electronic properties of the structure. Extended Hückel Theory (EHT), unlike HT which only utilizes the pz orbitals within the analysis, uses all of the available four orbitals, and is therefore a more thorough calculation that provides more information on the material. Additionally, Green's Function Theory and Landauer Formula are used in order to obtain conductance and local density of states (LDOS). Conductance and LDOS also provide information on the electrical properties of the structure.

1.2 Thesis Preview

This thesis will first peruse the theory in detail in Chapter 2. The theoretical models are Tight-Binding Model (TB Model) with Hückel Theory (HT), TB Model with Extended Hückel Theory (EHT), and Green's Function Theory. The results of these models include: electronic

band structure, density of states (DOS), conductance, and local density of states (LDOS). The calculations in order to obtain these results will be further discussed in detail in this chapter. After that, Chapter 3 displays the electronic band structure and DOS results. The chapter starts out with results for the band structure and DOS for AGNRs that are not functionalized. Then the band structure and DOS results for functionalized AGNR with H, N, O, F, P, S, and Cl are shown. First, band structure and DOS for the pure AGNR using HT and the pure AGNR using EHT will be displayed. Then, the band structure and DOS of functionalized AGNR with H, N, O, F, P, S, and Cl using EHT will be shown. Next, in Chapter 4, the discussion will turn to the conductance and LDOS results of those pure and impure structures. Similar to before, the conductance and LDOS of pure AGNR using HT and EHT will be presented first. Then, the conductance and LDOS for functionalized AGNR with H, N, and O will be shown. A summary in Chapter 5 will conclude this thesis.

Chapter 2: Theory: Band Structure, DOS, Conductance, and LDOS of GNRs

2.1 Introduction: Tight Binding Model and Green's Function Theory

One layer of graphite is graphene. Graphene is made of repeating carbons in a two-dimensional hexagonal arrangement. Carbon nanotubes (CNTs) and graphene nanoribbons (GNRs) can be formed from graphene. GNRs, an allotrope of carbon, are essentially strips cut from graphene that have a finite width, though are very long. Depending on how the GNR is cut, it can have different electronic properties and a different edge structure [19]. There are two specific edge structures: armchair and zigzag [30].

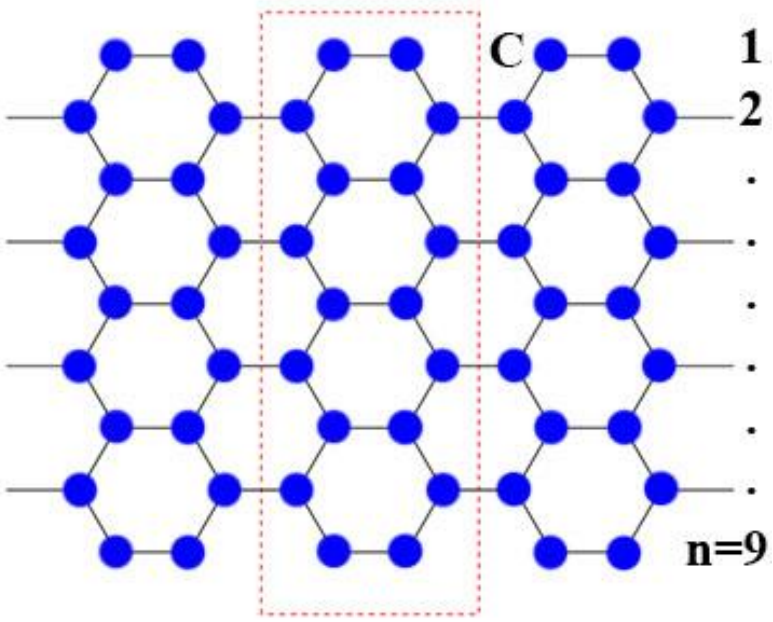

Figure 2.1: An n=9 dimer armchair graphene nanoribbon (AGNR).

Armchair graphene nanoribbons (AGNRs) are defined by the number of lines joining the atoms. These lines are called dimers. A schematic diagram of an AGNR is shown in Figure 2.1. The number of dimers is n=9 and the red-dashed box in this Figure shows the unit cell for the AGNR. Zigzag graphene nanoribbons (ZGNRs) are defined by the number of chains in the structure. Figure 2.2 shows a diagram of a ZGNR with n=6 chains. The black-dashed box in Figure 2.2 is the unit cell for the ZGNR. The carbon atoms are represented by the blue spherical objects at the vertices.

The unit cell repeats so it is only necessary to calculate the properties in one of the unit cells. In these hexagonal structures, each carbon atom has three nearest neighbors. The bond length is 1.42 Å between two carbon atoms [5, 30].

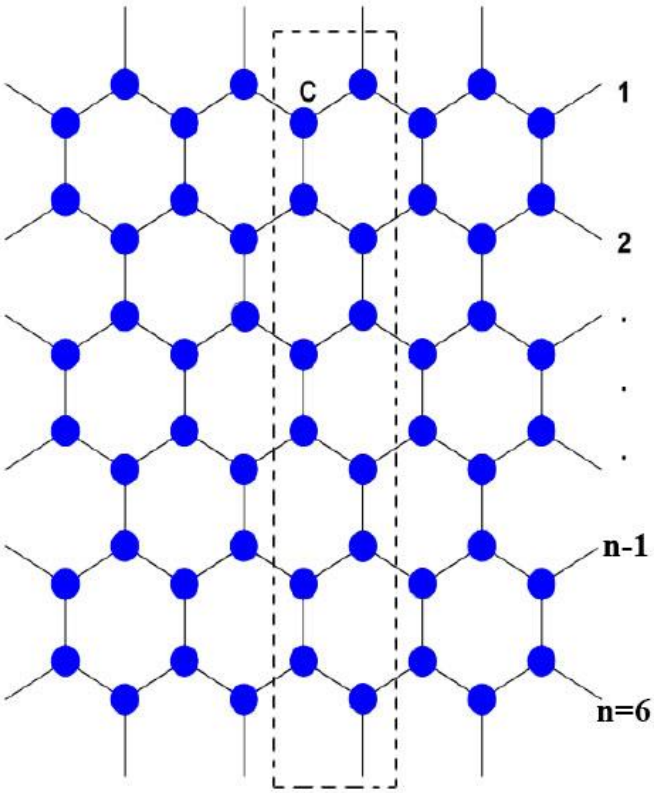

Figure 2.2: An n = 6 chain zigzag graphene nanoribbon (ZGNR).

Carbon is the sixth element in the periodic table and each carbon atom contains four electrons with the ability to form bonds. The electronic structure of carbon in the ground state is $1s^2 2s^2 2p^2$. $1s^2$ are the core electrons. These two electrons are strongly bound. The $2s^2 2p^2$ portion represents the valence electrons. The second shell orbitals are the ones responsible for forming bonds. In the excited state, one electron moves from the 2s orbital to the pz orbital. The 2s, $2p_x$, and $2p_y$ orbitals are orthogonal to each other and form sp^2 hybridized orbitals; these orbitals are 120° to each other [2, 5]. The sp^2 hybridized orbitals form σ bonds with each other and lie in a two-dimensional plane forming hexagonal arrangements. The pz orbitals lie perpendicular to the plane and the bond between pz orbitals is a π bond. σ bonds contribute to the arrangement of the structure and are strong, though the weaker π bonds mainly contribute to electron transport in the structure.

The theories used for calculating the electronic properties: electronic band structure, density of states (DOS), conductance, and local density of states (LDOS) will be discussed further in the following sections. The Tight Binding (TB) Model, the Hückel Theory (HT), and the Extended Hückel Theory (EHT) will be used for calculating the band structure and DOS. Whereas the Green's Function Theory will be used for calculating conductance and LDOS. The Landauer Formula is also utilized in obtaining the conductance.

By using the TB Model, one can obtain the Hamiltonian Matrix and, by solving the matrix, the energy band structure and DOS are obtained. The Hamiltonian matrix is constructed by using the Schrodinger Equation (SE). The total wavefunction is the linear combination of atomic orbitals (LCAO). The electronic band structure describes a range of energies an electron may have. DOS is essentially the number of electron states per unit volume per unit energy for a

certain energy value. HT uses the π bonds that are formed from the pz orbitals. EHT utilizes all of the available orbitals within the calculations. In order to obtain the details of the electronic properties of the structure, EHT with all the orbitals is used.

2.2 Tight Binding Model

The Tight Binding Model (TB Model) is a good approximation method that calculates the electrical properties of the structure. In the TB Model, electronic properties are calculated by considering only the nearest neighbor interactions in the system. The Hamiltonian of the TB Model is given by:

$$\mathbf{H} = \sum_i \epsilon_{ii} a_i^\dagger a_i \; + \sum_{<i,j>} V_{ij} a_i^\dagger a_j \;, \tag{2.1}$$

where ϵ_{ii} is the onsite energy, Vij is the overlap interaction energy between the nearest neighbors, and a_i and $a_j^\dagger$ are the creation and annihilation operators at i and j. The overlap interaction energy is also known as the hopping parameter relation. The sum of <i,j> restricts to only the nearest-neighbor atoms [5, 8, 31]. The onsite energy for the p orbitals in carbon is ε_p = -8.97 eV. The onsite energies are the diagonal terms in the matrix. The other matrix elements are composed of the overlap interaction energies combined with the phase factors.

The overlap interaction energy, otherwise known as the hopping parameter relation, is represented by [32]:

$$V_{ijk} = \eta_{ijk}\frac{\hbar^2}{\mathrm{m}d^2}. \quad (2.2)$$

Here, m is the mass of the electron, η_{ijk} is a dimensionless constant that depends on what sort of orbital it is, d is the distance between the neighboring nuclei, and the $\hbar$ is the Planck's constant. The value of d in this case is 1.42 Å, which is essentially the bond length between two neighboring carbon atoms. The i and j in the constant η_{ijk} represent either an s or p orbital and k represents either a σ or π bond. There are four different values of the constant η and they are listed in Table 2.1 [32]. The hopping parameter describes the coupling between orbitals that are neighboring [2, 32]. For example, in Table 2.1, the interaction energy constant between the two pz orbitals forming a π bond would be -0.81. The Hamiltonian matrix and hopping parameter equation are essentially what is needed to obtain the matrix elements.

Hopping Parameter (ηijk)	
$\eta ss\sigma$	-1.40
$\eta sp\sigma$	1.84
$\eta pp\sigma$	3.24
$\eta pp\pi$	-0.81

Table 2.1: The values for the constant η_{ijk} within the hopping parameter relation.

From this TB model, the electronic band structure is obtained by considering only the nearest neighbor interactions in the system. Band structure is the range of possible energies that an electron may have. The band structure shows the band gap and degeneracies of many bands [2]. For this specific application, Extended Hückel Theory (EHT) is used within the TB Model [3].

2.2.1 Hückel Theory

Hückel Theory (HT) is used within the Tight Binding (TB) Model, and is discussed in detail in this section. Only the pz orbitals are utilized within the HT calculation and only the nearest neighbor interactions are taken into account in the calculations. By using the TB Model, one can obtain the Hamiltonian Matrix, and the Hamiltonian Matrix is formed by using the Schrödinger Equation (SE). The SE is denoted as

$$\hat{H}\,\psi = E\,\psi, \tag{2.3}$$

where H is the Hamiltonian operator which takes the form $\hat{H} = \frac{-\hbar^2}{2m}\,\vec{\nabla}^2 + V\,(\vec{r})$ [33], $V(\vec{r})$ is the potential energy, and E is the total energy. Using orthogonality relations and scalar products, a series of equations are obtained and can be written as a matrix. The size of the matrix is dependent on the number of atoms in the unit cell of the chosen structure. By solving the matrix, eigenvalues and eigenfunctions are found [32].

The wavefunction, denoted as ψ in the SE, is written as a linear combination of atomic orbitals (LCAO) and this can be displayed as:

$$|\psi\rangle = \sum_i^N c_i|\varphi_i\rangle. \quad (2.4)$$

Here, c_i is a constant known as the probability amplitude of atom i, N is the total number of atoms in the unit cell, and φ_i is one of the atomic orbitals in the unit cell. The sum of this equation, which is the total wavefunction equation, is essentially the total number of orbitals of each atom in the unit cell. In basic Hückel Theory (HT), only the pz atomic orbitals are utilized in the calculation that obtains the electronic properties. The pz orbitals of a hexagonal structure are shown in Figure 2.3. The pz orbitals lie perpendicular to the plane with the positive lobe pointing upwards. The side view of two pz orbitals forming a π bond is shown to the left in the figure.

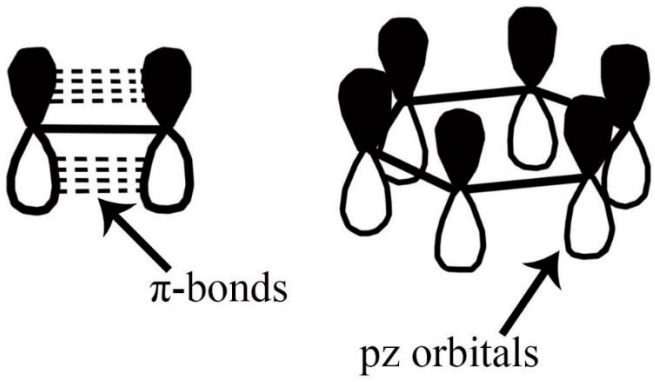

Figure 2.3: Pz orbitals on a hexagonal structure. The pz orbitals lie perpendicular to the plane. The positive lobes are represented by the solid black color. [34]

In order to show the detailed form of the wavefunction, we introduce a schematic structure for n=3 AGNR shown in Figure 2.4. Within the dotted lines of one unit cell, the atoms are numbered one through six starting from the top left carbon atom and ending at the bottom right carbon atom. This numbering scheme continues downwards if there are more atoms present in the system. For the n=3 dimer AGNR there are only six atoms in one unit cell. I is the unit cell in the middle, I-1 is the neighboring unit cell to the left of I, and I +1 is the unit cell to the right of I. The bond length between two carbon atoms is the lowercase letter a and it is 1.42 Å. The distance between the centers of each unit cell is 3a, where a is the bond length between the atoms. The lattice constant 3a is also the distance between the dotted-vertical lines, which represent the middle unit cell I shown in the figure. The system is symmetrical and the unit cell repeats.

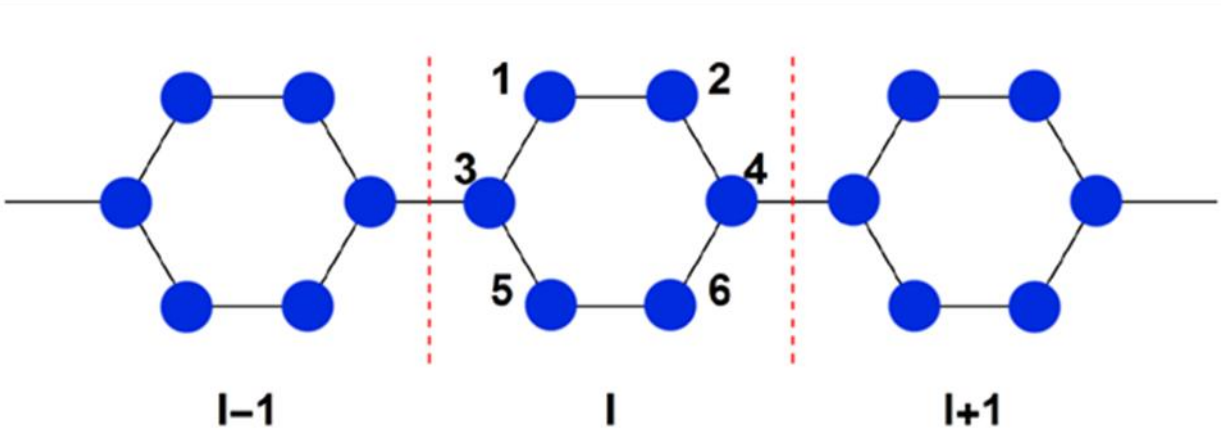

Figure 2.4: Illustration showing the unit cell I for an n=3 AGNR. The carbon atoms are numbered 1-6 starting at the top left atom. I-1 and I+1 are the neighboring unit cells to the left and to the right of unit cell I. [2, 5]

The total wavefunction in the unit cell I can be expressed as:

$$|\psi_I\rangle = \sum_{j=1}^{6} e^{i\vec{k}\cdot\vec{\tau_j}} c_j |\varphi_j\rangle. \quad (2.5)$$

In this equation, the phase factor has been introduced. j is the number of atoms in the unit cell, k is the wavevector, τ_j represents the position of an atom j. If the focus is on atom 1 in the I^{th} unit cell which is displayed in Figure 2.4, for example, then the rightmost portion adds all the interacting orbitals together. The complete orbital calculation utilizing HT has been discussed by previous researchers in our group [2, 3, 5, 34]. The EHT calculation is a more involved calculation than HT because all of the available orbitals are used within the analysis.

2.2.2 Extended Hückel Theory

Extended Hückel Theory (EHT) uses not only π bonds from the pz orbitals but also the s, px, and py orbitals forming different π and σ bonds [5]. In other words, all available orbitals are included in the EHT calculation. This calculation is more involved than the HT calculation, and the way that bonds form play a larger part. The different orbitals and bonds that form are shown in Figure 2.5. When certain orbitals bond, one or both of the orbitals move a certain angle. If the positive lobes are facing each other, then the resulting interaction energy will have a negative

value. The dark areas represent a positive lobe and the light areas represent a negative lobe. The pz orbitals lie perpendicular to the plane where the s, px, and py orbitals lie. Two p orbitals cannot form a bond if one is vertical and the other is in the horizontal direction. p orbitals form σ or π bonds depending on the angle, orientation of the orbitals, and whether it is bonding with an s or a p orbital. Additionally, two s orbitals only form σ bonds [32].

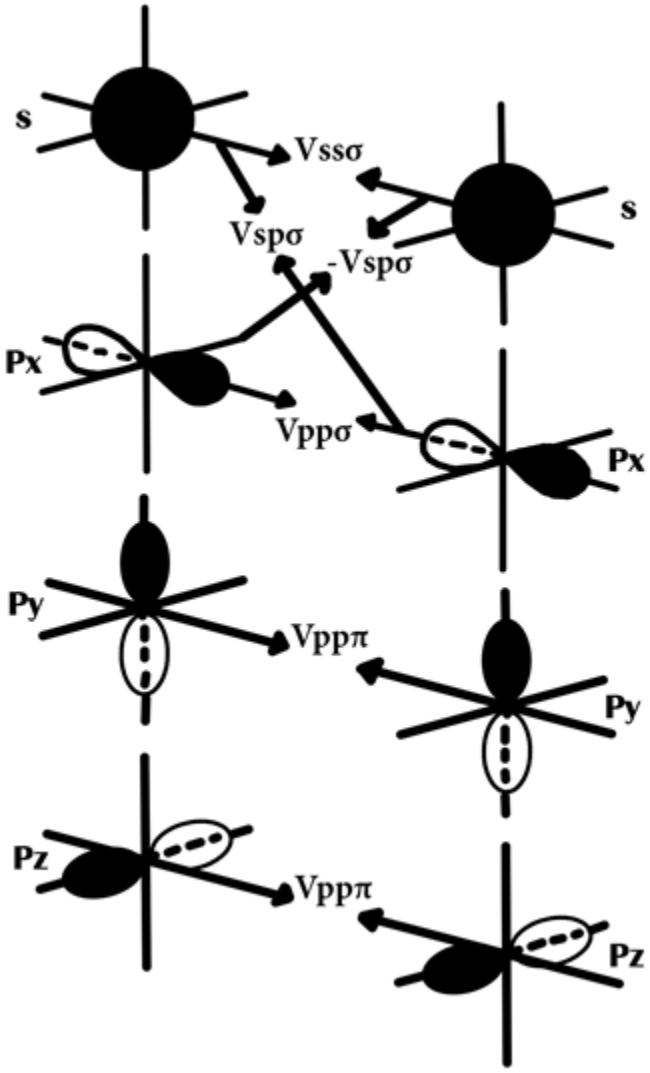

Figure 2.5: Illustration showing the different s, px, py, and pz orbitals and the different bonds that form. [32]

The structure in the more complex EHT calculation is similar to Figure 2.4. The only difference is that there are four orbitals in the calculations, not one orbital like with the HT calculation. A total wavefunction like Equation 2.5 is used. Building upon the wavefunction equation discussed in the previous section, the wavefunction equation in the EHT calculation for unit cell I can be written as:

$$|\psi_I\rangle = \sum_{j=1}^{6} e^{i\vec{k}\cdot\tau_j} \left[\alpha_1 |s_j\rangle + \alpha_2 |Px_j\rangle + \alpha_3 |Py_j\rangle + \alpha_4 |Pz_j\rangle \right] \quad (2.6)$$

The exponential term is the phase factor, k is the wavevector, τ_j represents the position of an atom j, and α is the probability amplitude. The probability amplitude is constant and is numbered up to 24, the same number of orbitals in unit cell I. In Equation 2.6, there are only 4 probability amplitudes because it is an equation that focuses on one atom. The number of atoms in the unit cell is 6. j varies over each atom in the unit cell. The scalar products of the orbitals are taken. For example, taking the scalar product for S_1, the s orbital of atom 1, looks like:

$$\langle s_1 | H | \sum_{j=1}^{6} e^{i\vec{k}\cdot\tau_j} \left[\alpha_1 |s_j\rangle + \alpha_2 |Px_j\rangle + \alpha_3 |Py_j\rangle + \alpha_4 |Pz_j\rangle \right] \rangle =$$

$$\langle s_1 | E | \sum_{j=1}^{6} e^{i\vec{k}\cdot\tau_j} \left[\alpha_1 |s_j\rangle + \alpha_2 |Px_j\rangle + \alpha_3 |Py_j\rangle + \alpha_4 |Pz_j\rangle \right] \rangle. \quad (2.7)$$

Adding every atom and orbital together expands Equation 2.7. The terms that are ultimately added together are only the nearest neighbors. This particular calculation focuses on atom 1 so the interaction terms with atoms 4, 5, and 6 are all zero. Eventually, the result of the analysis for the s orbital of atom 1 looks like:

$$\alpha_1 \varepsilon_s + e^{i\vec{k}\cdot\tau_{2-}\tau_1}[\alpha_2 E_{ss} + \alpha_2 P E_{sx}] + e^{i\vec{k}\cdot\tau_{3-}\tau_1}[\alpha_3 E_{ss} + \alpha_3 E_{sx} + \alpha_3 E_{sy}] = \alpha_1 \mathrm{E}. \quad (2.8)$$

The complete calculation for the s orbital of atom 1 is shown in Spencer Jones' thesis [5]. Repeating this process again for orbitals px, py and pz for atom 1, and all four orbitals for atoms 2, 3, 4, 5, and 6 in unit cell I produces all of the matrix elements. ε_s, is one such matrix element which represents the onsite energy; in this case it is the onsite energy of the s orbital. The onsite energy for the p and s orbitals are ε_{px} = -8.97 eV, ε_{py} = -8.97 eV, ε_{pz} = -8.97 eV, and ε_s = -17.52 eV [32]. There is no phase factor for the first term because it is the interaction with itself, not an interaction with another atom.

In this particular equation the E_{ss}, PE_{sx}, E_{sx}, and E_{sy} are the interaction, or overlap, energies between orbitals which represents another type of matrix element. These interaction energies are shown in more detail in Figure 2.6. The interaction energies are either positive or negative depending on the orientations of the lobes. These interaction energies are expressed in one hopping parameter or a combination of two hopping parameters. The hopping parameters are formed from Equation 2.2 and one of the four constants from Table 2.1.

$$E_{ss} = V_{ss\sigma} \qquad E_{xx} = \frac{1}{4}V_{pp\sigma} + \frac{3}{4}V_{pp\pi}, \qquad PE_{spx} = V_{sp\sigma}$$

$$E_{spx} = \frac{1}{2}V_{sp\sigma} \qquad E_{yy} = \frac{3}{4}V_{pp\sigma} + \frac{1}{4}V_{pp\pi} \qquad PE_{xx} = V_{pp\sigma}$$

$$E_{spy} = \frac{\sqrt{3}}{2}V_{sp\sigma} \qquad E_{xy} = \frac{\sqrt{3}}{4}V_{pp\sigma} - \frac{\sqrt{3}}{4}V_{pp\pi} \qquad PE_{yy} = V_{pp\pi}$$

$$E_{zz} = V_{pp\pi}$$

Figure 2.6: The interaction energies between orbitals [5, 32]

$\tau_2 - \tau_1$ in one of the exponential terms in Equation 2.8 is the displacement vector between the second and first atom. The exponential terms are the phase factors and these are shown in Table 2.3. The phase factors are denoted as g1, g2, g11, and g22 to more easily identify which phase factor it is when written in a matrix, for example.

Phase Factors	
g1	e^{ika}
g2	$e^{i\frac{ka}{2}}$
g11	e^{-ika}
g22	$e^{-i\frac{ka}{2}}$

Table 2.2: A Table that shows all of the four phase factors, where a is the bond length between two carbon atoms and k is the wavevector.

There are four possible values that phase factors can have. The phase factor describes the position in relation to some reference whether it be the center of the unit cell or a neighboring atom. In this case, it is the position in relation to a neighboring atom. The phase factor is negative if the distance from one atom to another is going from the right to the left.

2.2.3. Density of States

Both the band structure and the density of states (DOS) are obtained via diagonalizing the Hamiltonian matrix. The DOS reflects the band structure, and DOS is calculated from the band structure [2]. The DOS of the i^{th} band is given by:

$$DOS_i\ (E) = \frac{1}{2\pi} \int \delta\ [E_i(\vec{\boldsymbol{k}}) - \mathrm{E}]\mathrm{d}\vec{\boldsymbol{k}}, \tag{2.9}$$

Where, $\frac{1}{2\pi}$ is the normalization constant, $\mathrm{E_i}\,(\vec{\boldsymbol{k}})$ is the energy of band i, E is the energy of an electron, and $\vec{\boldsymbol{k}}$ is the wavevector, or momentum vector. The total DOS when all the bands are summed is written as:

$$DOS\ (E) = \sum_{i=1}^{N} \frac{1}{2\pi} \int \delta\ [E_i(\vec{\boldsymbol{k}}) - \mathrm{E}]\mathrm{d}\vec{\boldsymbol{k}}. \tag{2.10}$$

This delta function equation is summed from i=1 to i=N, summing over all the energy bands that are occupied.

In order to utilize the delta function in the equation above, there must be another, more efficient form which can be written as [2, 3]:

$$DOS(E) \cong \sum_i^N \frac{1}{2\pi} \sum_{\vec{k}} \frac{K_B T}{[E_i(\vec{k}) - \mathrm{E}]^2 + (K_B \mathrm{T})^2}, \quad (2.11)$$

where K_B is the Boltzmann constant and T is the absolute temperature. The Boltzmann constant is 8.617×10^{-5} eV·K^{-1}. In this research, T is a small value of 25 K. K_BT can be represented as η, a constant that is ultimately needed in order to calculate the conductance. The denominator terms represent energy. Low temperature displays the DOS as a continuum of sharp peaks, though higher energy displays the DOS as a smooth curve. The innermost summation is over a representative sample of k values and the outermost summation is from 1 to N. The delta function in the previous equation is replaced by a distribution function. This replacement is needed because computers cannot compute integrals very well [2, 3].

2.3 Green's Function Theory: Conductance and Local Density of States

Green's Function Theory is used in order to find conductance and local density of states (LDOS). In addition, the Landauer Formula helps obtain the conductance. Conductance is a measure of the ability of a substance to allow current to pass through. It is the reciprocal of

resistance. The LDOS, on the other hand, is the density of states of each individual atom in the system. Adding up all the LDOS results in the total density of states (DOS). LDOS gives details on the electron structures, and the electron transport that may or may not occur.

2.3.1 Conductance

The nanostructure during the conductance calculation is divided into three parts: the left lead, the conductor (also known as the molecule), and the right lead as shown in Figure 2.7. Conductance provides information on the electron transport of the structure, and the values are quantized. Typically the structure is semi-infinite along only one direction, but the width is finite.

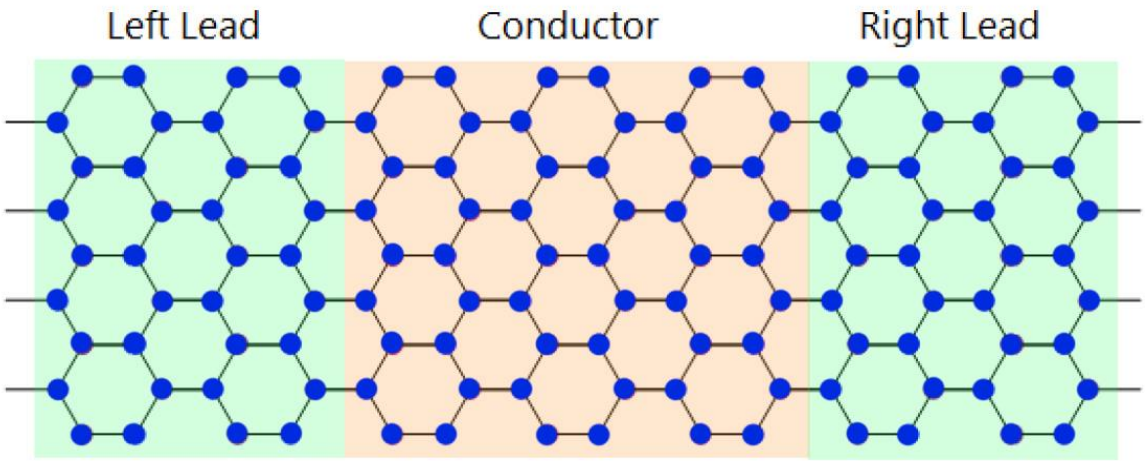

Figure 2.7: Illustration showing the conductor (the molecule), the right lead, and the left lead of a nanoribbon [3].

The leads and the conductor all have Hamiltonian matrices, and the largest matrix depends on the size of the conductor and left and right lead matrices [2]. The matrix for the conductor is HM, and this is shown in Figure 2.8 along with the matrices for the left and right leads, which are denoted as H1 and H2. HM1 and HM2 are the coupling matrices between the leads and the conductor. H11 and H22 are the coupling matrices between the unit cells in the left and right leads. In Figure 2.8, the conductor is orange and the left and right leads are red.

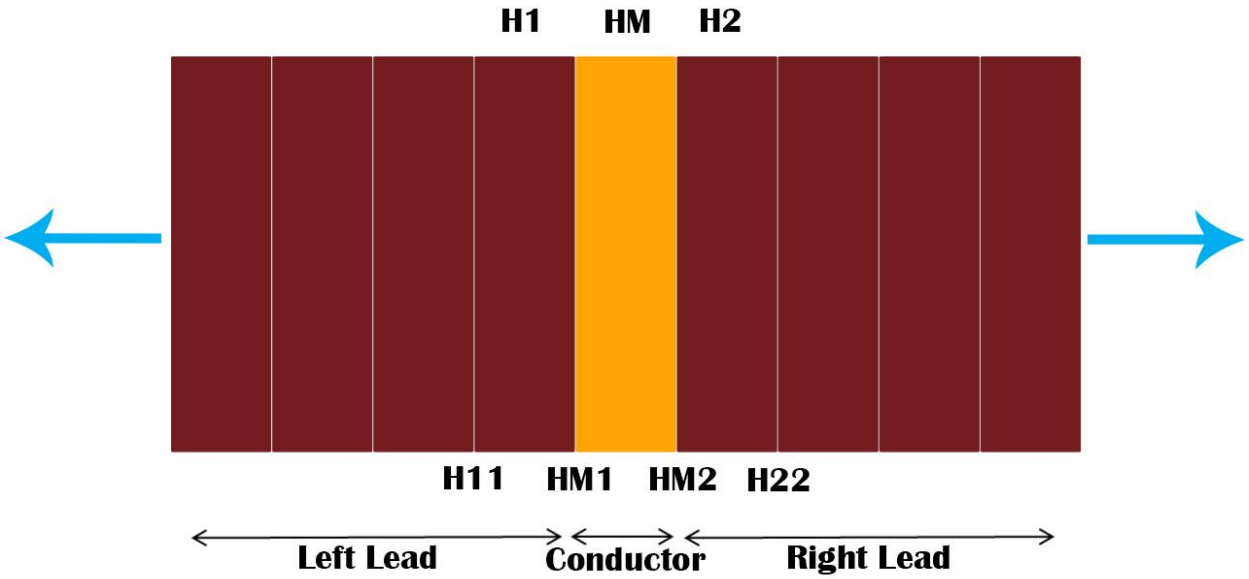

Figure 2.8: A more simplistic look at the whole structure showing the Hamiltonian Matrices for several sections. The conductor is orange and the leads are red. [2]

The total conductance equation, otherwise known as the Landauer Formula [1, 2, 8], can be written as:

$$G(E) = \frac{2e^2}{h} T(E), \tag{2.12}$$

where G is the total conductance and $T(E)$ is the transmission coefficient. G and T are functions of the total energy E of an electron. This conductance equation has a quantization of $\frac{2e^2}{h}$. Additionally, the transmission coefficient represents the probability that electrons coming into one end of the conductor will come out the other end as well [35]. The transmission coefficient depends on the total energy of an electron. It can be calculated from the Green's Functions, and can be expressed as [2, 8]:

$$T(E) = Trace\,[\Gamma_1 \cdot \boldsymbol{G_m} \cdot \Gamma_2 \cdot \boldsymbol{G_m}^{\dagger}]. \tag{2.13}$$

Here, $G_m^{\dagger}$ is the total advanced Green's Function and G_m is the total retarded Green's Function. The electrons of the advanced Green's Function are moving inward and the electrons of the retarded Green's Function are moving outward. The advanced Green's Function is the conjugate transpose of the retarded Green's Function. m is the mode. If m is 1 then it is to the left of the conductor, and if m is 2 then it is to the right of the conductor. Γ_1 and Γ_2 are the coupling functions of the leads to the conductor.

The total Green's Function is represented by the equation:

$$\boldsymbol{G_m} = [EI - H_c - \Sigma_1 - \Sigma_2]^{-1}, \tag{2.14}$$

where E is the total energy, I is the identity matrix, H_c is the Hamiltonian of the conductor, and Σ_1 and Σ_2 are the self-energy matrices. E can be expressed as $E = E_0 + i\,\eta$. The second, imaginary term is added to E_0, which helps the advanced Green's function grow very large [1, 2, 8]. This addition in the total energy expression is needed so that the inverse matrix does not diverge. This particular Green's Function is for the retarded Green's Function. The Advanced Green's Function is calculated from the conjugate transpose of this equation.

The left and right lead Hamiltonian matrices are defined in terms of the self-energy matrices. The coupling function matrices, which are calculated through the iterative process and from the self-energy matrices, are represented by the formulas [1-3, 8]:

$$\Gamma_1 = i\,[\Sigma_1 - \Sigma_1^{\dagger}],$$

$$\Gamma_2 = i\,[\Sigma_2 - \Sigma_2^{\dagger}], \qquad (2.15)$$

where Σ_1 and Σ_2 are the self-energy matrices from the left and right leads. The self-energy matrices are obtained by doing several iterations. The potential felt by electrons due to interactions with its surroundings is accounted for because of self-energy [3]. The self-energy matrices are found by [2, 8]:

$$\Sigma_1 = HM_1^{\dagger} \cdot \boldsymbol{G_1} \cdot HM_1,$$

$$\Sigma_2 = HM_2 \cdot \boldsymbol{G_2} \cdot HM_2^{\dagger}. \qquad (2.16)$$

Here, HM1 and HM2 are the coupling matrices between the conductor and left and right leads. G1 and G2 are the Green's Functions for the left and right leads of the structure.

The left and right lead Green's Functions are found from the following two formulas [8]:

$$\mathbf{G_1} = [EI - H1 - H11^{\dagger} \cdot \tilde{T}]^{-1},$$

$$\mathbf{G_2} = [EI - H2 - H22 \cdot T]^{-1}, \qquad (2.17)$$

where I is the identity matrix, H1 and H2 are the Hamiltonian matrices for the left and right leads, H11 and H22 are the coupling matrices between the unit cells in the left and right leads, and E is the total energy. The T and $\tilde{T}$ are the transfer matrices. The transfer matrices are two equations that are discussed in more detail in Li, et al [8]. It is calculated from the Hamiltonian Matrix elements using an iterative process [8]. Recursion formulas are also used in calculating the transfer matrices.

2.3.2 Local Density of States

Once Green's function is calculated, the local density of states (LDOS) can be found. LDOS gives details on the electron structures, and the electron transport that may or may not occur. The LDOS can be found by using [1, 2, 8]:

$$LDOS_i(E) = -\frac{1}{\pi}\ Im\ [\boldsymbol{G_m}(i,\ i)]. \tag{2.18}$$

This is essentially the LDOS of atomic site i in the conductor that is obtained from the Green's Function of individual atoms. G_m is the total retarded Green's Function, and i is the ith diagonal element in the Green's Function. Similar to DOS, LDOS shows the number of states at a certain energy. Though, unlike DOS, LDOS shows only the number of possible energy states at a certain energy times the probability that an electron in those energy states can be measured to be on one given atom. All of the LDOS added together is the total DOS. The DOS is calculated from:

$$DOS\ (E) = \frac{-1}{\pi}\ Im[Trace[\boldsymbol{G_m}]]. \tag{2.19}$$

This formula obtains the total DOS by summing up all the sites. Equations 2.19 and 2.9 produce the same results.

2.4 Summary

The theories used to calculate band structure, density of states (DOS), conductance, and local density of states (LDOS) were discussed in detail in this chapter. Tight Binding (TB) Model, Hückel Theory (HT), and Extended Hückel Theory (EHT) are utilized to produce the band structure and DOS results. In the TB Model interactions were restricted to only the nearest neighbors. Only the pz orbital was considered for the HT calculation, though all four orbitals

were considered for the EHT calculation. The s, px, py, and pz orbitals form either σ or π bonds depending on the direction the orbitals are facing and depending on the orbitals that are bonding. The interaction energies that result from those bonds are either negative or positive depending on which lobes are facing each other [32].

By solving the Hamiltonian Matrix, the electronic band structure and DOS are obtained. Green's Function Theory, with the help of the Landauer Formula, produces the conductance for the structure. Conductance portrays the electron transport that may or may not occur at certain energies in the system. LDOS is also calculated using Green's Function, ***Gm***. LDOS is the density of states for each individual atom in the structure. The total DOS is the sum of all individual LDOS. In summary, with the assistance of TB Model, HT, EHT, Green's Function Theory, and Landauer Formula, electronic and transport properties of GNRs are calculated.

Chapter 3: Results: Band Structure and DOS of Functionalized AGNRs Using Extended Hückel Theory

3.1 Introduction

This chapter will primarily present the band structure and density of states (DOS) results for armchair graphene nanoribbons (AGNRs) using Extended Hückel Theory (EHT). Band structure graphs are typically Energy vs. k (the wave number) and DOS graphs are usually Energy vs. DOS. DOS always reflects the band structure, and DOS is obtained from the band structure.

First, the band structure and DOS results for pure n = 3 dimer AGNR using Hückel Theory (HT) will be presented in the following section. Then, the band structure and DOS results for n = 3 AGNR using EHT will be observed. Pure and impure AGNR, which are terminated with H, N, O, F, P, S, and Cl, will be discussed in detail at that moment. Only the nearest neighbor interactions are taken into account when doing the HT and EHT calculations. HT only uses pz orbitals, though EHT uses all of the four available orbitals in the calculation.

Band structure is important because it provides a lot of information about the electronic properties of the structure. In order to address the issues related to the electronic properties of a solid material a general illustration of a band structure is presented in Figure 3.1. The lowest bands are filled first with electrons, and a total of two electrons may occupy each band. Valence bands are the filled bands below Fermi energy, and conduction bands are the unfilled bands

above Fermi energy. Fermi energy is centered in the middle around 0 eV. The band gap is the gap between the valence and conduction bands and it is centered in the middle.

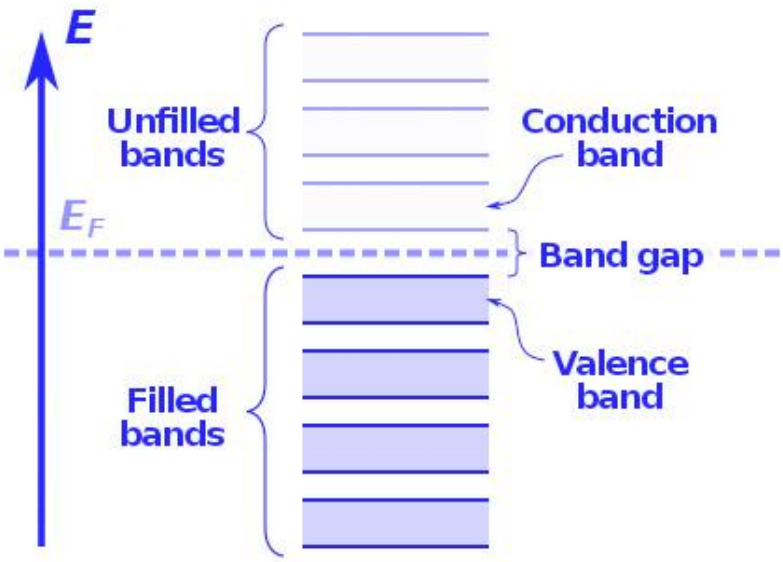

Figure 3.1: Illustration showing the conduction bands, the valence bands, the band gap, and the Fermi energy level (E_F).

Quantum confinement creates a band gap in AGNRs that depends on the width of the ribbon [36]. If there is no band gap then the material is metallic. If the band gap is greater than 4 eV, then the material is an insulator and if it in somewhere in the middle then the material is a semiconductor [3]. The dimer rule for an AGNR exhibiting semiconducting behavior is n= 3p for an odd number of dimers and n= 3p+1 for an even number of dimers. The rule for metallic AGNRs, on the other hand, is n= 3p+2. p in the dimer rule relation is an integer and n is the

number of dimers [5, 28, 37-39]. This project focused on n=3 dimer AGNRs so the structures exhibit semiconducting behavior.

3.2 Electronic Band Structure and DOS of Perfect AGNRs

An AGNR with no edge termination is a pure structure with no imperfections like with the functionalized AGNRs. There are dangling bonds at the edge. Adding another element to the edge terminates those bonds. This will be discussed further in the next section. In this particular research project, our main focus is to study the electronic properties of functionalized AGNRs using EHT. In the following sub-sections, the electronic properties of a perfect AGNR using HT and EHT will be presented. These results will ultimately be compared to the functionalized results shown in Section 3.3.

3.2.1 Electronic Band Structure and DOS Using Hückel Theory

The electronic band structure and density of states (DOS) for a pure n=3 AGNR using HT are shown in Figure 3.2. There are only six atoms in the unit cell, which is shown in Figure 2.4. Since HT utilizes only the pz orbitals, it is expected there will be six bands in the electronic band structure. Band structure is plotted as a function of wavevector k. The relation between the electron energy and the wavevector for a free particle is given by

$$E = \frac{\hbar^2 k^2}{2m}. \quad (3.1)$$

Here, E is the electron energy, m is the mass of the electron, k is the wavevector, and $\hbar$ is Planck's constant. If the band is parabolic, then the electrons freely propagate. Though, if the bands are flat, then the denominator is very large. The effective mass of the electron is very heavy [3].

The six bands in the band structure in Figure 3.2 are symmetrical about Fermi energy at 0 eV. There are three conduction bands above Fermi energy and three valence bands below Fermi energy. There are non-conducting bands at $\pm$3 eV. Non-conducting bands are flat bands, also known as stationary states, where the effective mass of the electron is near infinite, and the electron cannot move very easily. Curved bands are areas where the mass is not extremely high so the electron moves more freely. The band gap is located in the middle between the conduction band edge and the valence band edge showing that the structure is semiconducting because it is greater than 0 eV and less than 4 eV across. The band gap is around 2.3 eV wide. Giving enough energy to an electron in the valance bands helps the electron jump over the band gap to the conduction bands.

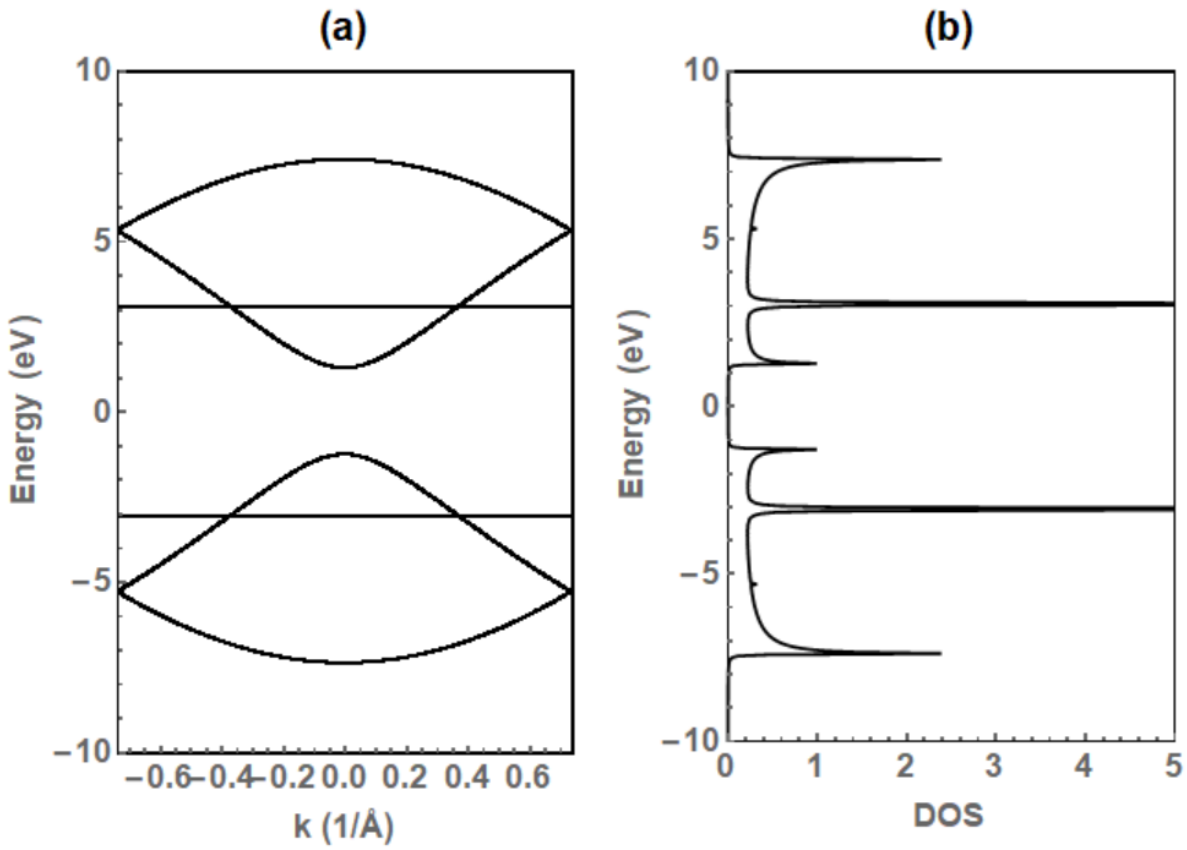

Figure 3.2: (a) The band structure and (b) the density of states of a perfect n=3 AGNR using HT.

The DOS reflects the band structure and it essentially tells which areas are the most likely energy states that the electron will be in when it moves. It shows the number of possible states at certain energy values. DOS is calculated from the band structure, and is plotted as a function of energy. Larger peaks in the DOS show that there is a higher chance that an electron will be at that specific energy. The high peaks in the DOS reflect the flat bands in the band structure. In addition, the band gap at ± 1 eV in Figure 3.2 has no bands in the band structure or peaks in the DOS.

3.2.2 Electronic Band Structure and DOS Using Extended Hückel Theory

The electronic band structure and density of states (DOS) of a pure n=3 dimer AGNR using Extended Hückel Theory (EHT) is shown in Figure 3.3. There are 24 bands in the band structure that come from the s, px, py, and pz orbitals of the 6 carbon atoms in the unit cell. The number of orbitals can be obtained by the relation 8n where n is the number of dimers.

Unlike pure AGNR using Hückel Theory (HT), the conduction and valence bands are not symmetric about Fermi energy, which is located around 0 eV. There are more flat bands below Fermi energy. As stated before, flat bands are non-conducting bands, and the group velocity of the electrons is near zero [5, 8, 37]. Therefore, the effective mass of the electrons are near infinite. Flat bands are due to the s, px, and py orbitals of carbon [5]. The weaker π bonds are represented by the flat bands near Fermi energy. Similar to the pure AGNR using HT, there is a gap between the lowest conduction band and the highest valence band so this material is exhibiting semiconducting behavior. This is to be expected because of the dimer rule that states that AGNRs are semiconducting when n=3p, for odd n values. p is an integer. The band gap is around 2.5 eV wide.

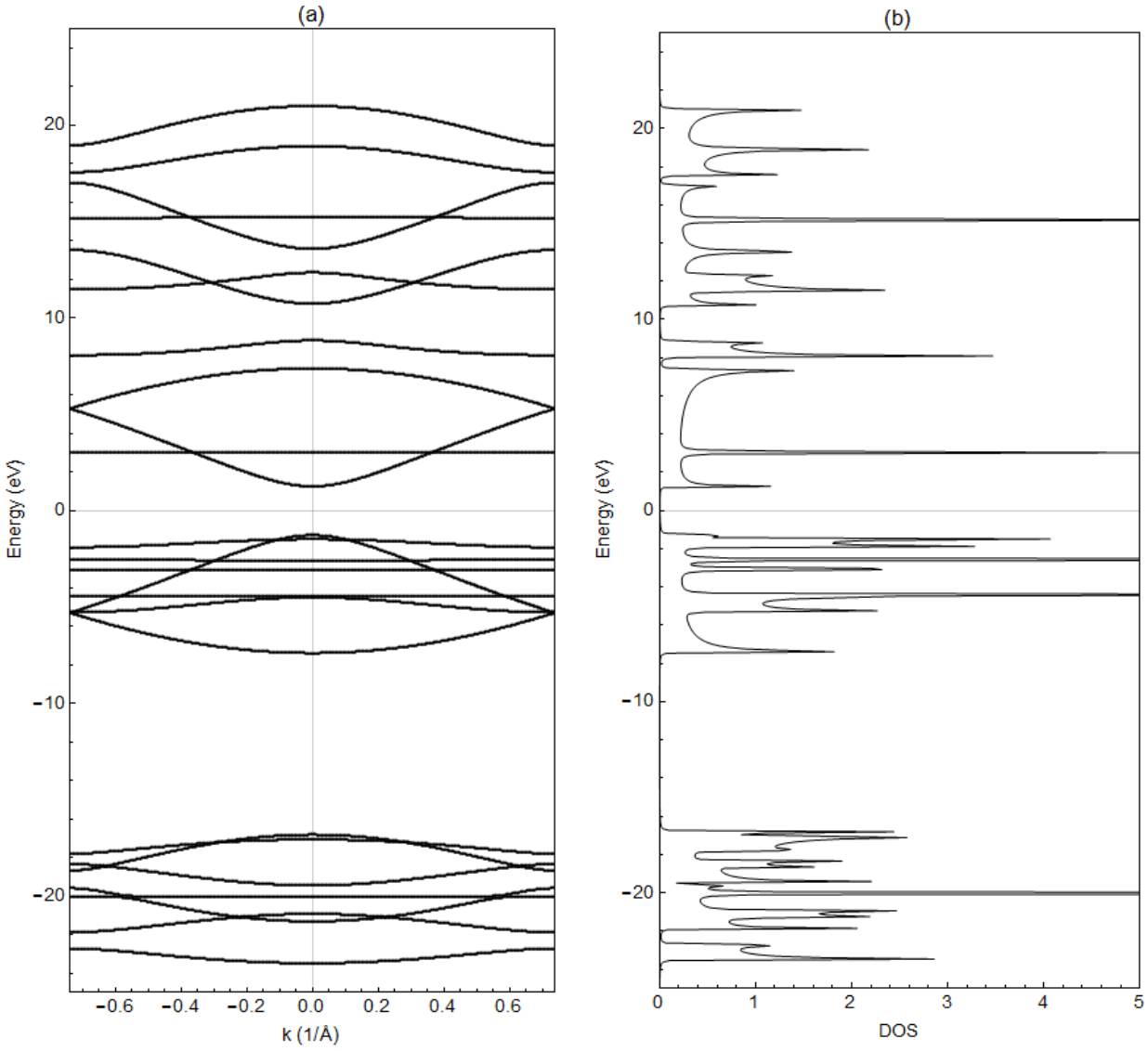

Figure 3.3: (a) The band structure and (b) the density of states of a perfect n=3 AGNR using Extended Hückel Theory.

DOS is essentially the number of k points per energy value. Wherever there is a flat band in the band structure, there is a tall peak in the DOS in Figure 3.3. In other words, there is a high probability that an electron will be there at that energy. There are no peaks in the DOS around

Fermi energy and there are no bands in the band structure at the band gap. The DOS reflects the band structure and does not have peaks where there are no bands.

As stated before, the band structure is asymmetric for pure AGNR using EHT, and there are extra bands below Fermi energy. The calculations for the band structure and the DOS results for pure AGNR using EHT, shown in Figure 3.3, shows the existence of edge, or non-bonding, orbitals from the dangling edge atoms C1, C2, C5, and C6 so there are extra valence bands near Fermi energy [5].

3.3 Electronic Band Structure and DOS of Functionalized AGNRs

The focus of this research dealt with n = 3 functionalized AGNR, which is shown in Figure 3.4. This figure shows a single unit cell of the AGNR, not the whole AGNR like what is displayed in Figure 2.4. The blue circles are carbons and the yellow circles are some element that terminates the edges. The dangling edge bonds from the element that is added in creates localized edge states [40]. This research project functionalized the edges with the elements H, N, O, F, P, S, and Cl. These elements were chosen because they naturally bond with carbon and form various compounds.

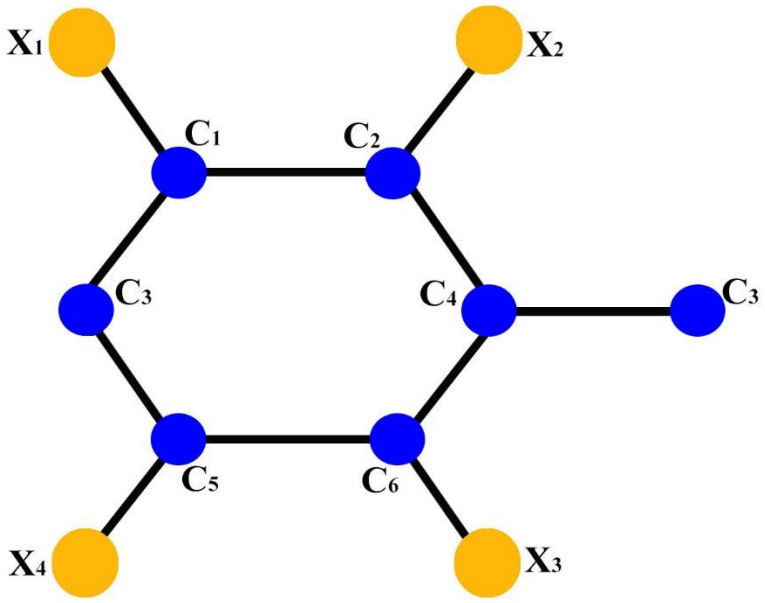

Figure 3.4: Diagram showing an n=3 AGNR terminated with an element X.

The bond length between two carbons is 1.42 Å, as mentioned in Chapter 2. Though, the bond length between carbon and another element is different depending on what element it is. This is displayed in Table 3.1. The bond lengths are taken from various online chemistry tables and from previous researchers in the group [3, 5].

Atoms That are Bonded	Bond Length (Å)
C-H	1.09
C-C	1.42
C-N	1.47
C-O	1.43
C-F	1.32
C-P	1.87
C-S	1.82
C-Cl	1.77

Table 3.1: Bond lengths between carbon and some other elements.

To obtain the number of carbon atoms like in Figure 3.4 for example, use the relation 2n where n is the number of dimers. In order to obtain the total number of orbitals in the system, the number of orbitals in one carbon is multiplied by the number of carbon atoms. For an n = 3 AGNR with 6 carbon atoms and 4 orbitals in each atom, there will be 24 total orbitals. The matrix size for a pure AGNR using EHT will therefore be 24 x 24. This can be expressed as the relation 2n * 4, which can also be written as 8n. The relation changes for structures that have edge termination. For example, when AGNR is terminated with Cl, there is only one orbital that contributes to the calculations and there are four chlorine atoms at the edges of the structure so the equation becomes 8n + 4. Therefore, the total number of orbitals for an AGNR that is terminated with Cl is 28.

Atom	Onsite Energy of s and p Orbitals (eV)
Hydrogen	-13.6
Carbon	-8.97
Nitrogen	-11.47
Oxygen	-14.13
Flourine	-16.99
Phosphorus	-8.33
Sulfur	-10.27
Chlorine	-12.31

Table 3.2: The onsite energies for the s and p orbitals of various atoms.

A structure is a pure structure until functionalization occurs, then it is impure. Edge functionalization is the focus of this research. The various elements used in edge termination have different onsite energies than carbon. Table 3.2 shows the different onsite energies for the s and p orbitals of various atoms that functionalize the edges [32]. The onsite energy for hydrogen is for the s orbital. The rest of the values are all onsite energies for the p orbitals. It is also important to note that the onsite energy for the s orbital of carbon is also used, and that is at a value of -17.52 eV. The following section will display the band structure and DOS results for functionalized AGNRs in order of increasing atomic number.

			Orbital Diagram			
Atomic Number	**Element**	**Electron Configuration**	s	px	py	pz
1	H	$1s^1$	↑			
6	C	$\mathbf{1s^2}2s^2 2p^2$	↑	↑	↑	↑
7	N	$\mathbf{1s^2 2s^2} 2p^3$		↑	↑	↑
8	O	$\mathbf{1s^2 2s^2} 2p^4$		↑↓	↑	↑
9	F	$\mathbf{1s^2 2s^2} 2p^5$		↑↓	↑↓	↑
15	P	$\mathbf{1s^2 2s^2 2p^6 3s^2} 3p^3$		↑	↑	↑
16	S	$\mathbf{1s^2 2s^2 2p^6 3s^2} 3p^4$		↑↓	↑	↑
17	Cl	$\mathbf{1s^2 2s^2 2p^6 3s^2} 3p^5$		↑↓	↑↓	↑

Table 3.3: Atomic numbers, elements, and their electronic and spin configurations. The electron configurations of the core electrons which do not participate in forming bonds are shown in bold font.

The atomic number is equal to the number of electrons in an element, and it determines the properties of an element. Details on the various elements that are utilized in this research are shown in Table 3.3. The table includes the electron configuration, which is the distribution of electrons of an atom, or a molecule, in an atomic, or molecular orbital. The section in boldface of the electron configuration in the table represents the core electrons, and the sections not in boldface are the valence electrons. As previously stated in Chapter 2, the core electrons are strongly bound. However, the valence electrons participate in forming bonds. The table also includes the orbital diagram which is a pictorial depiction of the valence electrons. The electrons follow Hund's Rule that states that each shell is first occupied with an electron of one spin, and then adding an electron of the opposite spin, not doubly occupied at once. All electrons in singly occupied orbitals have the same spin. Also, due to Pauli Exclusion Principle, which states that no

two electrons can occupy the same state, there can only be an electron with spin up and an electron with spin down orientation in a shell. Wherever there are single electrons, that particular orbital affects the calculations. For example, only the pz orbital affects the calculation when Cl is involved.

3.3.1 Electronic Band Structure and DOS of a Functionalized AGNR: H, N, O, F, P, S, and Cl

An AGNR that is terminated along the edge is no longer a pure structure, but an imperfect structure. Terminating the edge with another element adds more orbitals to the total, and alters the electronic properties of the structure, which is reflected in the band structure and DOS. One purpose of adding another element at the edge is to help protect the material from deformations, which changes the materials' properties [3]. The following results discuss n=3 AGNRs for edge termination with H, N, O, F, P, S, and Cl.

Functionalized AGNR with H

In Figure 3.5, the band structure and the density of states (DOS) are shown for an AGNR that is terminated with hydrogen using Extended Hückel Theory (EHT). The bond length between hydrogen and carbon is 1.09 Å. There are 28 total orbitals in a unit cell for this structure. The four extra orbitals come from the hydrogen atoms attached to the edges near C1, C2, C5, and C6 as illustrated in Figure 3.4. Figure 3.5 (a) displays 28 bands in the band structure. The bands are more symmetric around the Fermi energy level. There are fewer bands around the Fermi

energy, and more bands at lower energies showing that the bands are more tightly bound at lower energies. As previously mentioned, the s orbital is hybridized with the other orbitals. Carbon creates a strong covalent bond with hydrogen, and the bands at the lower energies represent these features [41-44]. The bands at lower energies are therefore due to strong σ bonds and are tightly bound, and the bands closer to the Fermi energy are due to the weaker π bonds and contribute to conduction [5]. Figure 3.5 (b) shows similar changes to the DOS due to the edge termination with hydrogen. There are fewer peaks around the Fermi energy and more peaks far from the Fermi energy. There are many more peaks at the lower energies which represent the σ bonds. The bandgap centered around the Fermi energy does not have any peaks and still shows that the material exhibits semiconducting behavior. The band gap is approximately 2.6 eV wide. In conclusion, the band gap has not changed significantly as observed for the perfect structure.

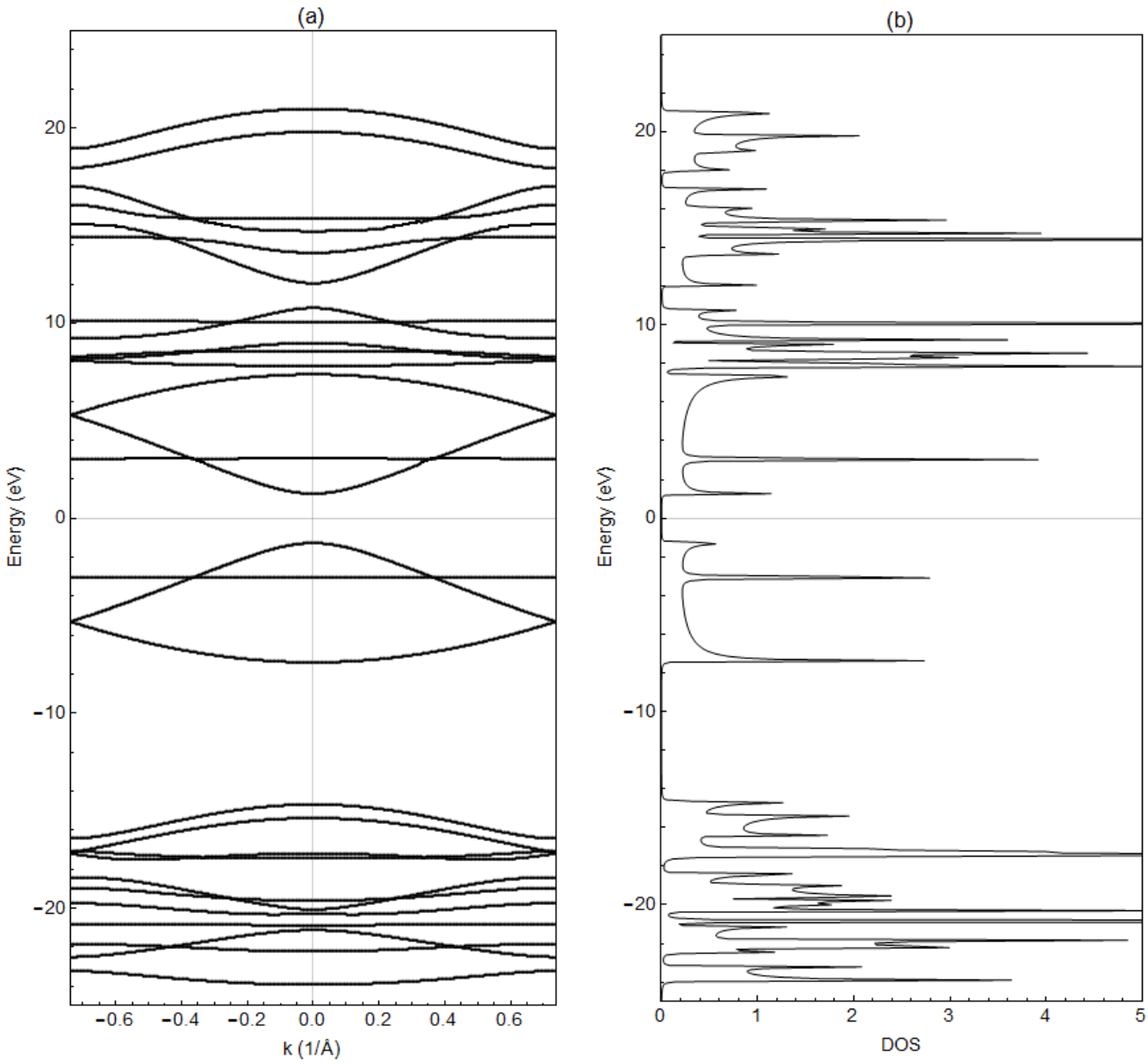

Figure 3.5: (a) The band structure and (b) the density of states of an n=3 AGNR with hydrogen edge termination.

Functionalized AGNR with N

Figure 3.6 displays the band structure and DOS of an AGNR edge terminated with N. The bond length between a carbon atom and nitrogen atom is 1.47 Å. In this case, the unit cell has 36 total orbitals. The px, py, and pz orbitals from the four nitrogen atoms contribute to the formation of both σ and π bonds and these bonds are included in the calculation. Unlike the H functionalized structure, there are 12 extra new bands shown in Fig. 3.6 (a). Interestingly, the highest valence band is closer to Fermi energy. In addition, there is a large number of stationary states at around +10 eV in the band structure which are tightly bound. The new bands from -10 to -16 eV show a high number of states in some places that previously were not present in the pure structure. The band gap is about the same as the perfect structure results, which is around 2.2 eV. The band gap has decreased when compared to the perfect structure. Though, the structure is still semiconducting. There are many new possible states that are observed at specific energies in the DOS result shown in Figure 3.6 (b).

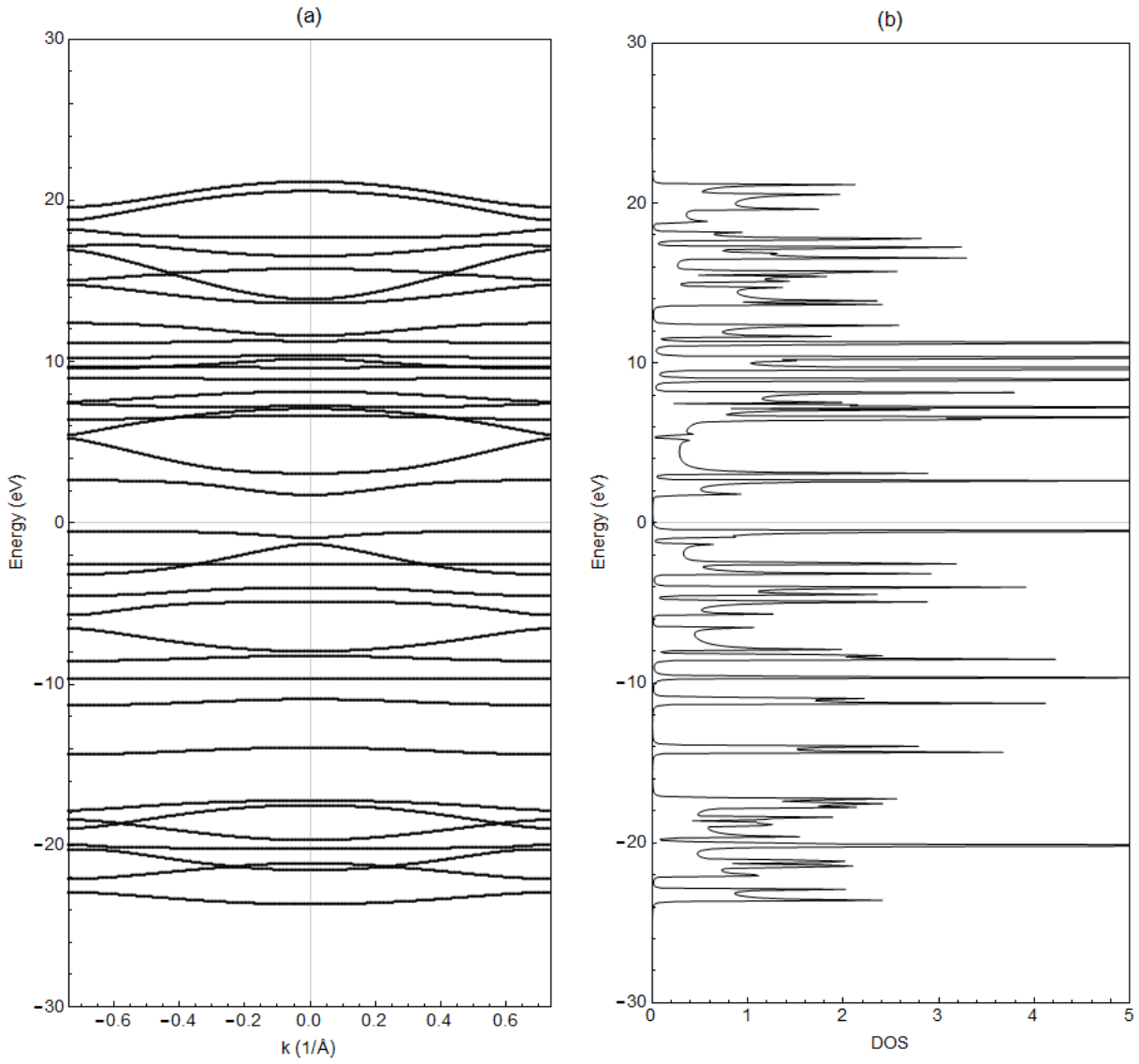

Figure 3.6: (a) The band structure and (b) the density of states of an n=3 AGNR with nitrogen edge termination.

Functionalized AGNR with O

The band structure and DOS for an AGNR edge terminated with oxygen is displayed in Figure 3.7. The bond length between an oxygen and a carbon atom is 1.43 Å, which is very close to the bond length value between two carbon atoms. Only the py and pz orbitals from the four oxygen atoms contribute to the calculation. Figure 3.7(a) displays the energy bands as a function of wavevector. As a result, there are 8 extra orbitals added to the structure. Hence, 32 orbitals are included in the calculation. There are new stationary states that appear in several places. These bands appear below the Fermi Energy and around +10 eV. The bands above +10 eV do not cross as much as the bands in that area in the pure AGNR band structure. Many of these bands are also diminished in curvature. In addition, there are more gaps in the DOS peaks where there are no states. Like the previous termination the band gap is around 2.2 eV wide. As with the previous edge termination, the band gap after edge termination with oxygen decreases. It is still a semiconductor.

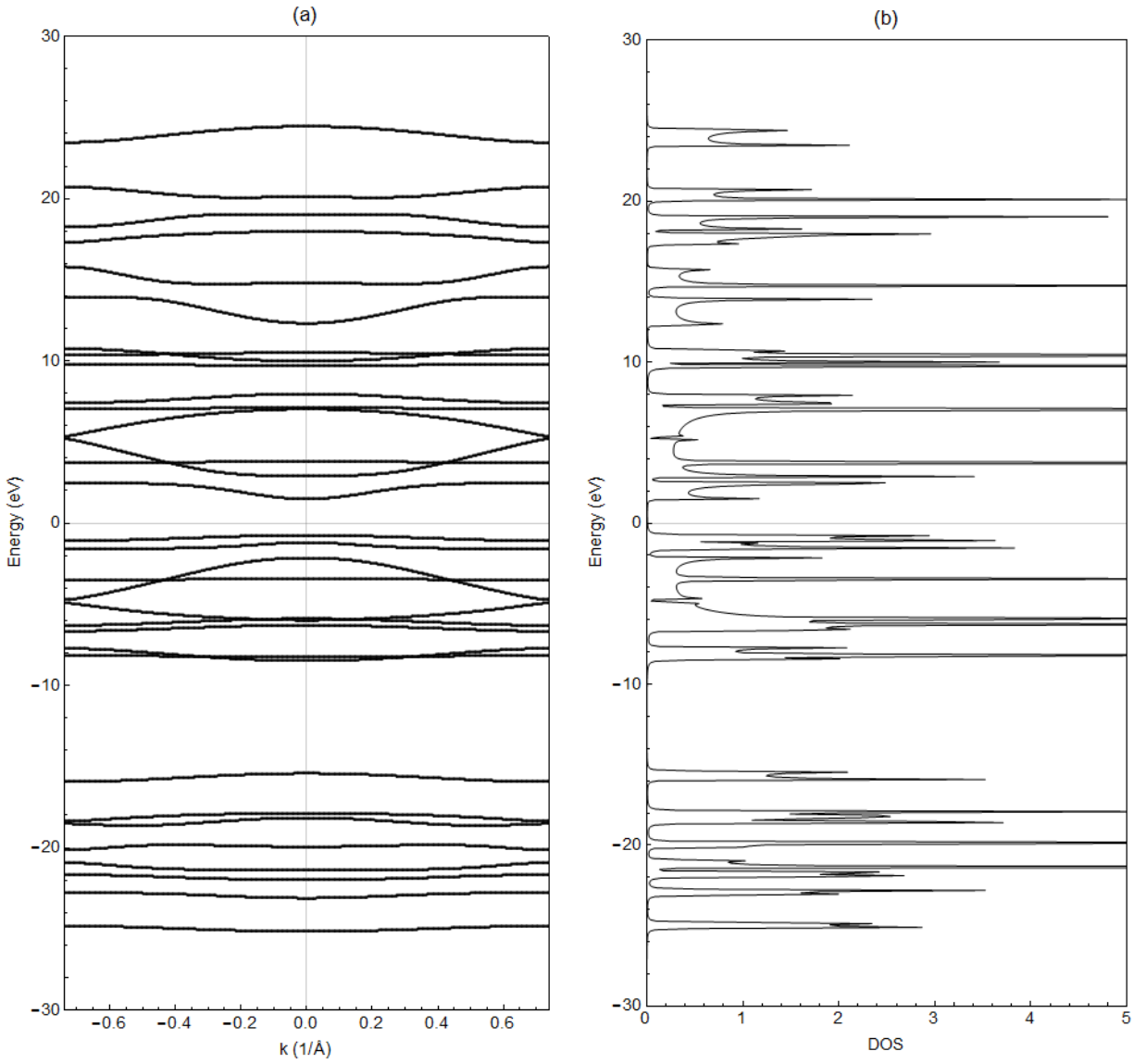

Figure 3.7: (a) The band structure and (b) the density of states of an n=3 AGNR with oxygen edge termination.

Functionalized AGNR with F

Figure 3.8 shows the band structure and DOS of an AGNR edge terminated with fluorine. The bond length between the carbon and the fluorine atom is 1.32 Å. Similar to H edge termination, this structure has 28 orbitals and 28 energy bands. Only the pz orbital from each of the four fluorine atoms contributes to the calculation. The bands at high and low energies are very similar to the pure structure. Similar to AGNR that is functionalized with H, there is an increase in flat bands around the Fermi energy. In addition, there are now flat bands around -3 eV and -10 eV in the valence band region. Consequently, there are more possible states for electrons in the DOS in this area too. There is now a high probability that an electron will be found at and around these particular energies. The band gap, when compared to the perfect structure, is about the same at around 2.5 eV wide. Though, the structure is still exhibiting semiconducting behavior. In summary, modulations or changes are observed due to the presence of fluorine at the edges of the structure.

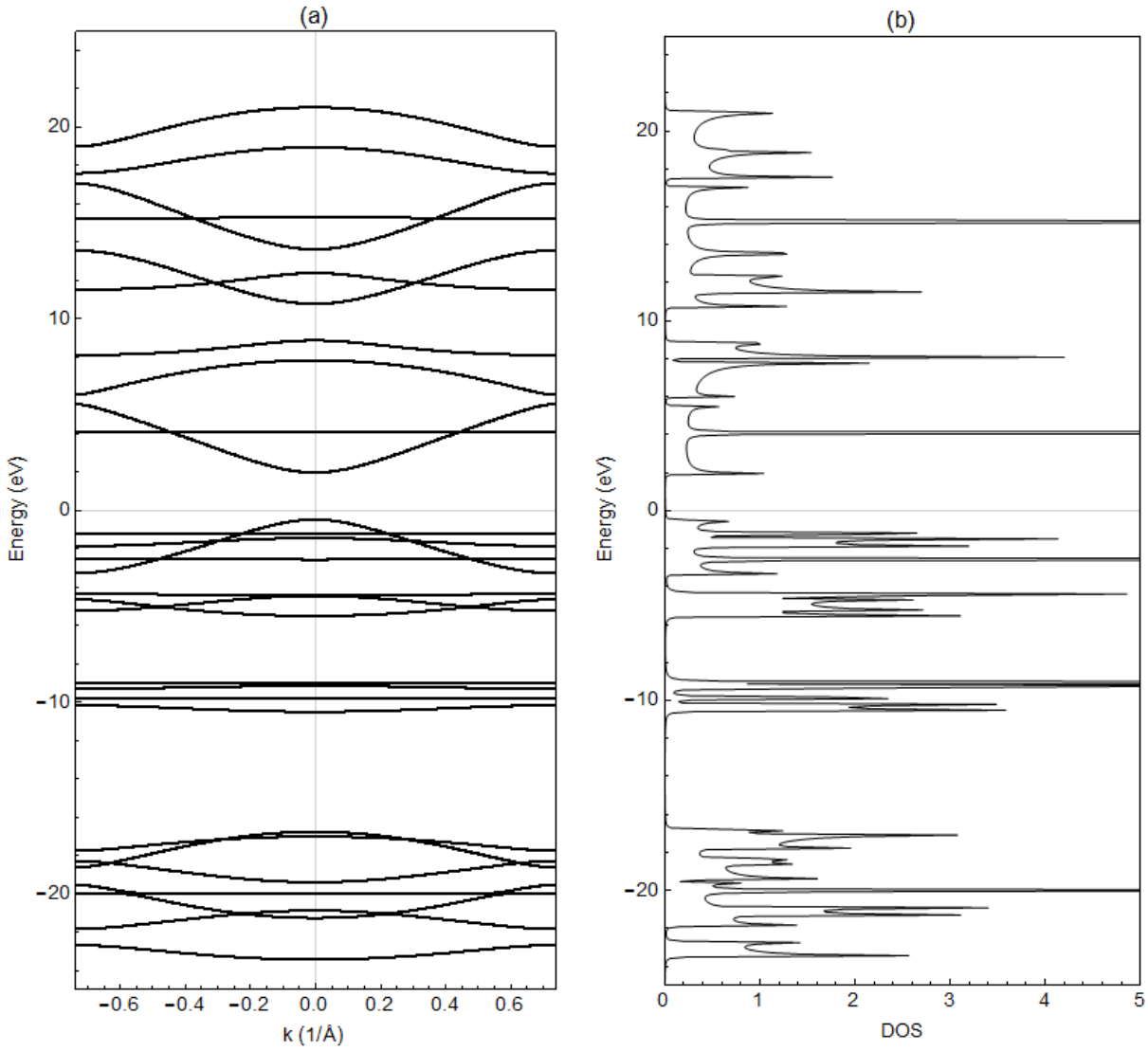

Figure 3.8: (a) The band structure and (b) the density of states of an n=3 AGNR with fluorine edge termination.

Functionalized AGNR with P

Figure 3.9 shows the band structure and DOS for an AGNR edge terminated with phosphorus. The bond length between a phosphorus and a carbon is 1.87 Å. Like N edge termination, this structure has 36 total orbitals. The extra 12 orbitals come from the phosphorus at the edges. The px, py, and pz orbitals contribute to the calculation from the four phosphorus atoms. Therefore, one expects 36 energy bands in Figure 3.8 (a). It is imperative to note that there are more flat bands around +10 eV in the conduction band region, and more possible states in the DOS too. There are many tightly bound states in this area. The effective mass of the electrons in this area are very high so the electrons do not move very well. In addition, there are some flat valence bands above -10 eV that conversely contribute to more possible states in the DOS graph. Interestingly, intertwining bands are now located at the Fermi energy, which were not in the pure structure. The lowest conduction band is now on the Fermi energy. The band gap is approximately 0 eV. This material is exhibiting metallic behavior rather than semiconducting behavior.

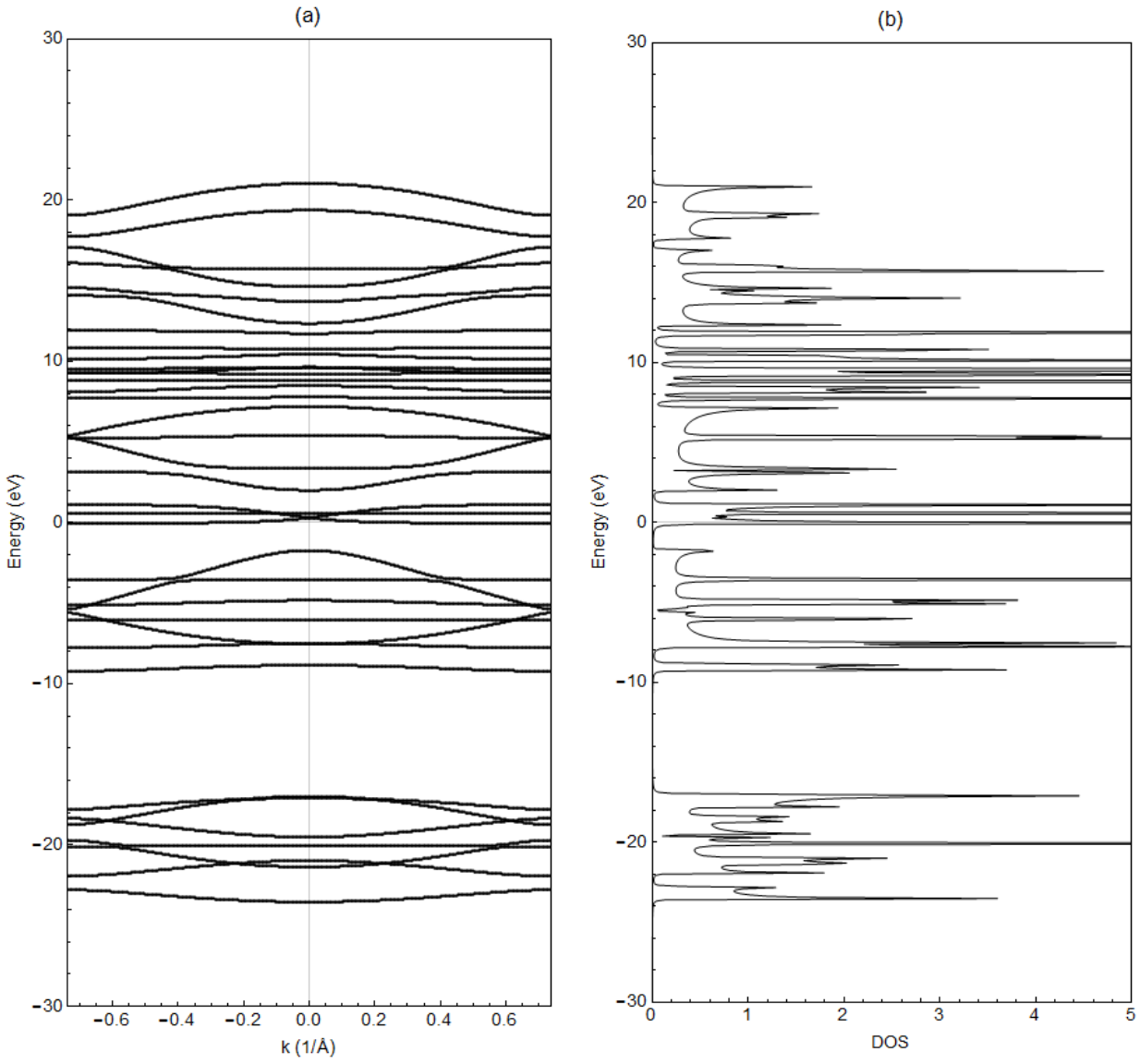

Figure 3.9: (a) The band structure and (b) the density of states of an n=3 AGNR with phosphorus edge termination.

Functionalized AGNR with S

The band structure and DOS for an AGNR edge terminated with sulfur in shown in Figure 3.10. Energy bands are plotted as a function of wavevector, and DOS are plotted as a function of electron energy. The bond length between a carbon and a sulfur is 1.82 Å. Like the O edge termination, this structure has 32 total orbitals. The 8 extra py and pz orbitals are from the four sulfur atoms. There are few similarities with this band structure and the energy band structure of the pure AGNR. The bands are distributed across all areas. There are also many flat bands. Conversely, there are more possible stationary states for electrons, as shown in the DOS. It is also interesting to note that above +10 eV in the conduction band region, there is less intertwining between some bands. Also, the highest valence band is nearly at Fermi energy. The band gap in this structure is smaller than the previous results. It is approximately 1.7 eV across. This band gap, when compared to the perfect structure, has decreased in size. The material it is still a semiconductor.

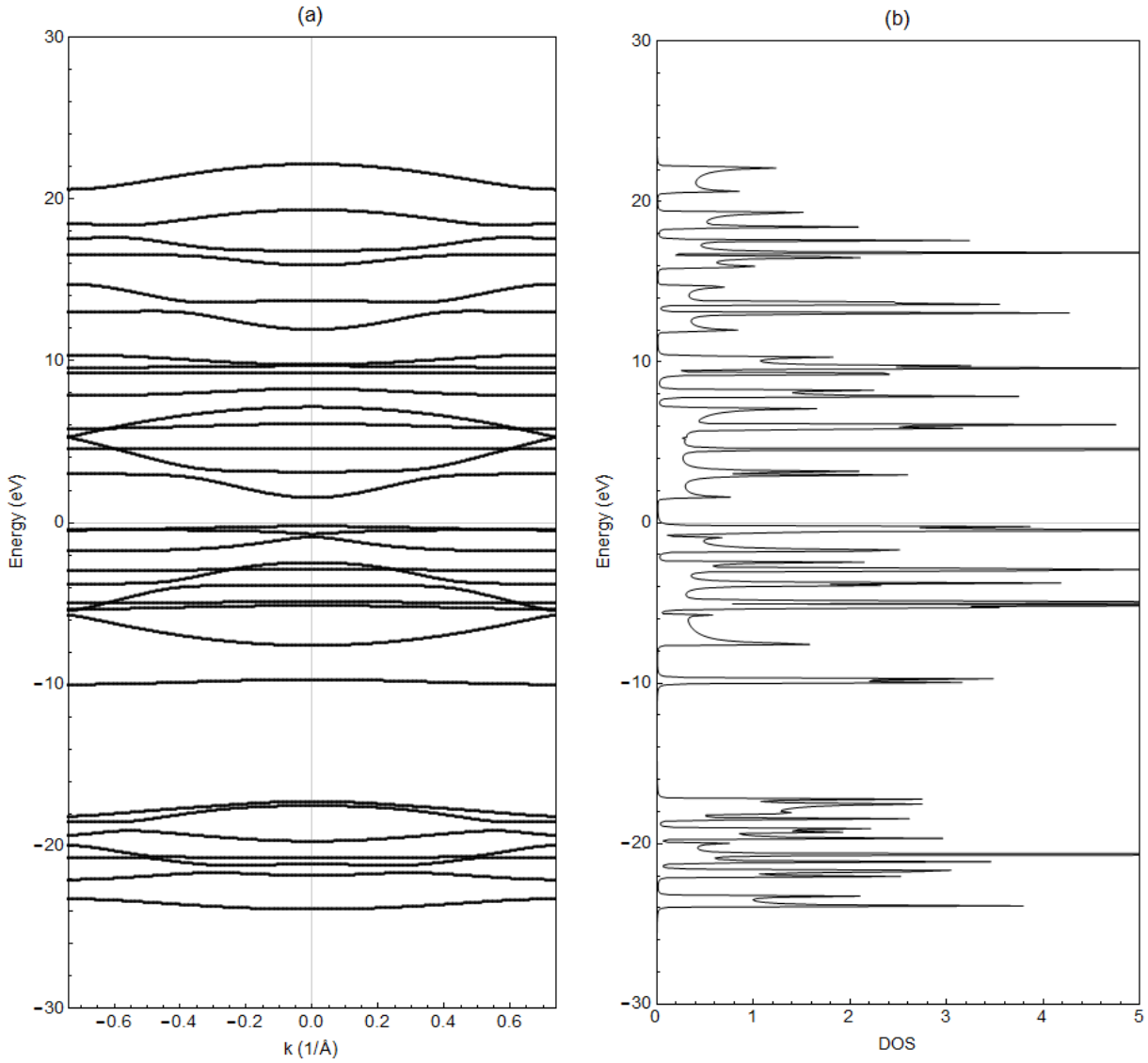

Figure 3.10: (a) The band structure and (b) the density of states of an n=3 AGNR with sulfur edge termination.

Functionalized AGNR with Cl

Figure 3.11 shows the band structure and DOS for an AGNR edge terminated with chlorine. The bond length between a chlorine and a carbon atom is 1.77 Å. Similar to H and F edge termination, this structure has 28 total orbitals, and 28 energy bands in Figure 3.11 (a). Only a pz orbital from each of the four chlorine atoms contributes to the calculation. The band structure for the AGNR terminated with Cl mostly stays the same when compared to the pure structure, though this is not the case for the area around the Fermi energy level where there is a large increase in tightly bound flat, valence bands. The electrons in this region have high effective masses and cannot move very well. These are due to stationary states. The conduction bands above the Fermi energy level have almost the same pattern as the perfect structure. The same can be said about the valence bands at very low energies. Conversely, there is a larger amount of states in Figure 3.11 (b) around that portion. The highest valence band is closer to the Fermi energy showing that the band gap has shifted by a small amount upwards. It is concluded that the material is still semiconducting with a band gap of approximately 2.2 eV. The band gap has decreased when compared to the pure structure.

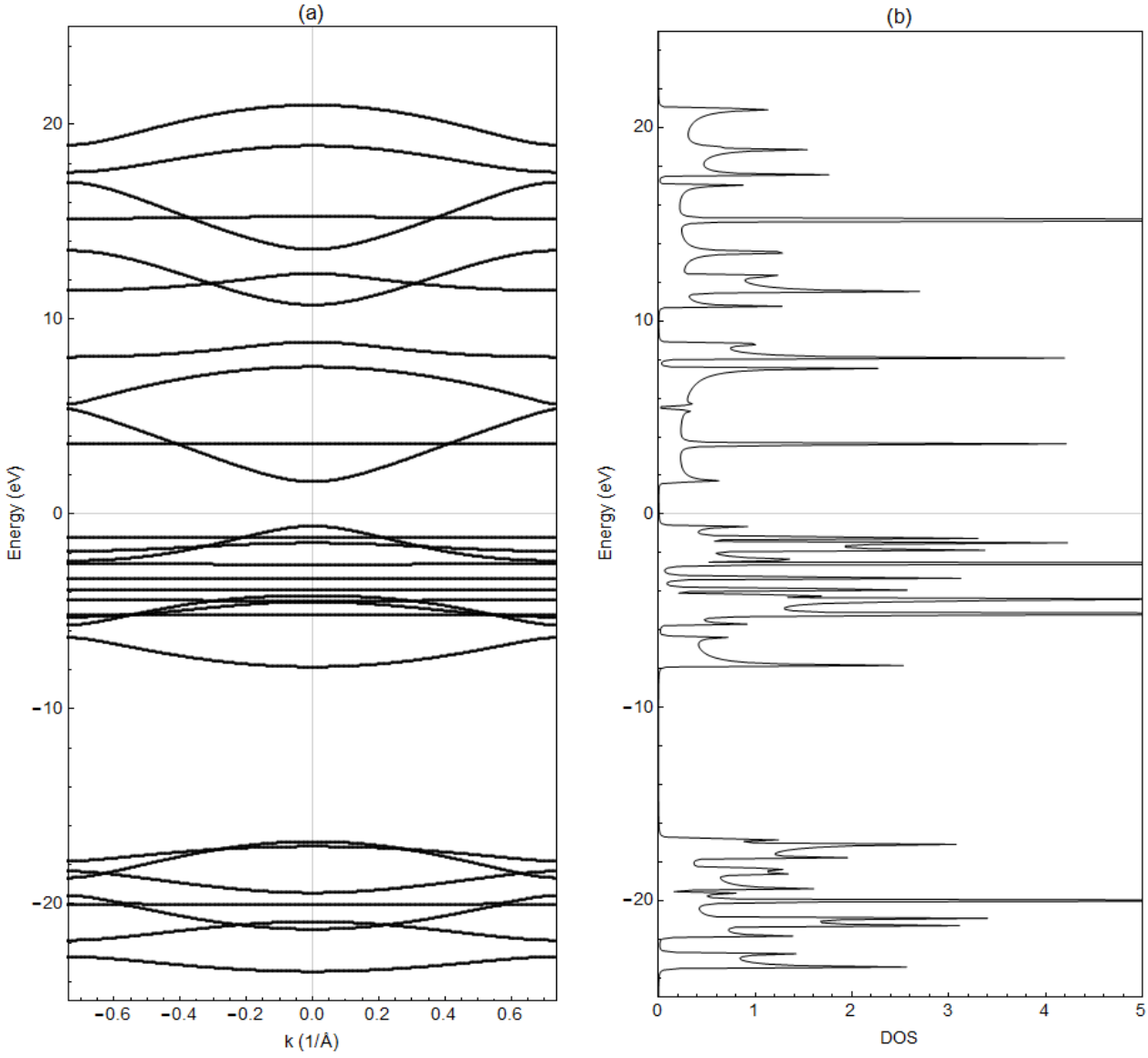

Figure 3.11: (a) The band structure and (b) the density of states of an n=3 AGNR with chlorine edge termination.

The summary of the band gap of the functionalized AGNRs is shown in a tabular form here.

Atomic Number	Element	Band Gap (eV)
1	H	2.6
7	N	2.2
8	O	2.2
9	F	2.5
15	P	0
16	S	1.7
17	Cl	2.2

Table 3.4: A Table that displays all of the band gaps of the functionalized AGNRs.

The band gap for the perfect AGNR using EHT is 2.5 eV. One may notice from Table 3.4 that the band gap is strongly dependent on the bond length between the carbon and the functionalized element. Here, it is found that hydrogen has the highest band gap value at around 2.6 eV. The bond length between a carbon and a hydrogen is 1.09 Å. Phosphorus has the lowest band gap value at approximately 0 eV. The bond length between a carbon atom and a phosphorus atom is 1.87 Å. It can be observed that the size of the band gap is related to the bond length. The bond length between carbon and hydrogen is the lowest, and the bond length between carbon and phosphorus is the highest value. In other words, higher bond length values result in a shorter band gap, and lower bond length values result in a longer band gap. Shorter bond lengths are

stronger than longer bond lengths. Longer bond lengths break more easily, and the structures with longer bond lengths have smaller band gaps.

3.4 Summary

This chapter primarily discussed functionalized n=3 AGNRs using EHT results. The band structure and DOS results for each case were presented. Pure AGNR using HT was shown. Then, pure AGNR using EHT was displayed. After that, results for a functionalized AGNR with H, N, O, F, P, S, and Cl using EHT were perused in detail. The perfect AGNR using EHT and the functionalized AGNR using EHT results were compared.

Pure AGNR using HT is symmetric about the Fermi energy for both the band structure and the DOS. However, pure AGNR using EHT was not symmetric. The symmetry is due to the pz orbitals. Because of the edge orbitals in the EHT calculation not being accounted for, edge functionalization is done in order to fix this. Almost all of the results showed semiconducting behavior which follows the dimer rule that n=3p for odd n values, where p is an integer. Though, P edge functionalization was more metallic than a semiconductor. There were a few functionalized structures where the band gap decreased in size. It was found that a higher bond length results in a smaller band gap, and a lower bond length results in a larger band gap.

Chapter 4: Conductance and Local Density of States

4.1 Introduction

This chapter will go over conductance and local density of states (LDOS) in great detail. The conductance and LDOS for pure n=3 AGNR using Hückel Theory (HT) and Extended Hückel Theory (EHT) will be shown first. Then, the conductance and LDOS for n=3 AGNR using EHT functionalized with H, N, and O will be displayed.

Conductance is plotted against energy. As mentioned previously in Chapter 3, electron conduction mainly relies on the pz orbitals. The strong σ bonds are tightly bound unlike the weaker π bonds. Comparing conductance and band structure shows how much electron transport occurs by however many bands cross. Higher multiples of conductance, or electron transport, relates to more bands crossing at a particular energy.

Additionally, it is easy to see on conductance graphs whether the band gap has changed or not. Similar to the band structure and DOS results, if there is no gap, then the material is metallic. There are no modes of electron transport at the band gap for a materials that are not metallic. This project focused on n=3 AGNR so the structures should follow the dimer rule where n=3p for an odd n value and where p is an integer. By that rule, the materials are semiconductors. As discussed previously in Chapter 2, Landauer Formula and Green's Function Theory are used in order to find the conductance for the system [37].

LDOS shows the individual density of states for each atom in the system. LDOS values are smaller than the total DOS values. This is because LDOS is only one part of a whole. Adding

up all of the LDOS produces the total DOS. LDOS is typically displayed in a group similar to how the atoms are arranged in the system. The system, in this project, looks like what is shown in Figure 2.4. There is longitudinal and horizontal symmetry that can be observed when the LDOS graphs are displayed as a group. LDOS not only shows the individual density of states for each atom in a system, but also gives the details on the electron structures and the electron transport that may occur. Additionally, it shows the number of possible energy states at certain energies. Green's Function is utilized in order to find the LDOS of a system.

4.2 Conductance and LDOS of AGNR

Conductance and LDOS for pure n=3 AGNR using HT and EHT will be shown first in the following section. Then, the conductance and LDOS for n=3 AGNR using EHT functionalized with H, N, and O will be displayed in a later section. Transport properties of a material is characterized by conductance. LDOS is essentially the density of states for each individual atom and gives details on the electron structures and the electron transport that occurs. Due to symmetry, the LDOS for atoms 1, 2, 5, and 6 are identical for a system comprised of carbons. Additionally, the LDOS for atoms 3 and 4 are also identical to each other. Only the LDOS for atoms 1 and 3 will be shown.

4.2.1 Conductance and LDOS for Pure n=3 AGNR Using Hückel Theory

Figure 4.1 presents the conductance for an n=3 pure AGNR using HT [5]. Comparing the conductance and band structure shows the same number of bands crossing at a specific energy as

how many multiples of conductance, otherwise known as the modes of transport, are at that particular area. For example, in Figure 4.1 there is only one multiple value of conductance at 3 eV so there would only be one band crossing at that energy in the band structure. The bands are seen as modes of transport for electrons in the structure [3].

There are no modes of transport at the band gap, and one can easily observe that this structure is a semiconductor and the band gap is approximately 2.3 eV. The conductance at the band gap is zero. Conductance is quantized by $\frac{2e^2}{h}$. This is taken from the Landauer equation, which was discussed in Chapter 2, and the values are written as integer multiples of $\frac{2e^2}{h}$. The conductance in Figure 4.1 is at the first multiple of that value after ± 1 eV.

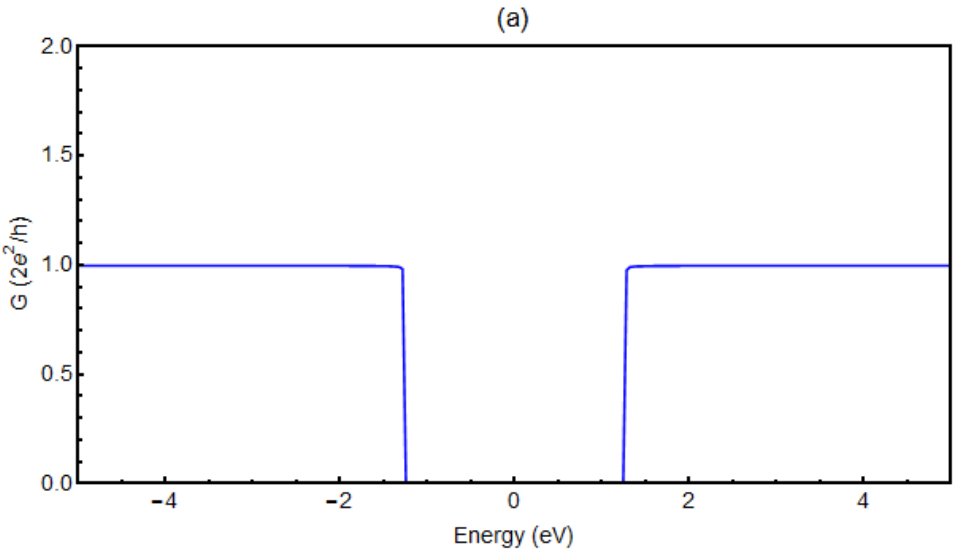

Figure 4.1: The conductance for pure n=3 AGNR using Hückel Theory [5].

The LDOS for the perfect AGNR using HT is shown in Figure 4.2 [5]. LDOS shows which individual atom contributes to transport at certain energies. The number of states per energy is displayed in the LDOS. The LDOS is typically displayed in a group similar to the setup of the structure in Figure 2.4 starting with atom 1 at the top left and ending with atom 6 at the bottom right. The LDOS is similar to the total DOS, though the peaks are smaller. There is a stationary state at ± 3 eV in the LDOS for atoms 1, 2, 5, and 6. It is clear that due to the symmetry of the structure, the LDOS for atoms 1, 2, 5, and 6 are identical, and atoms 3 and 4 are identical.

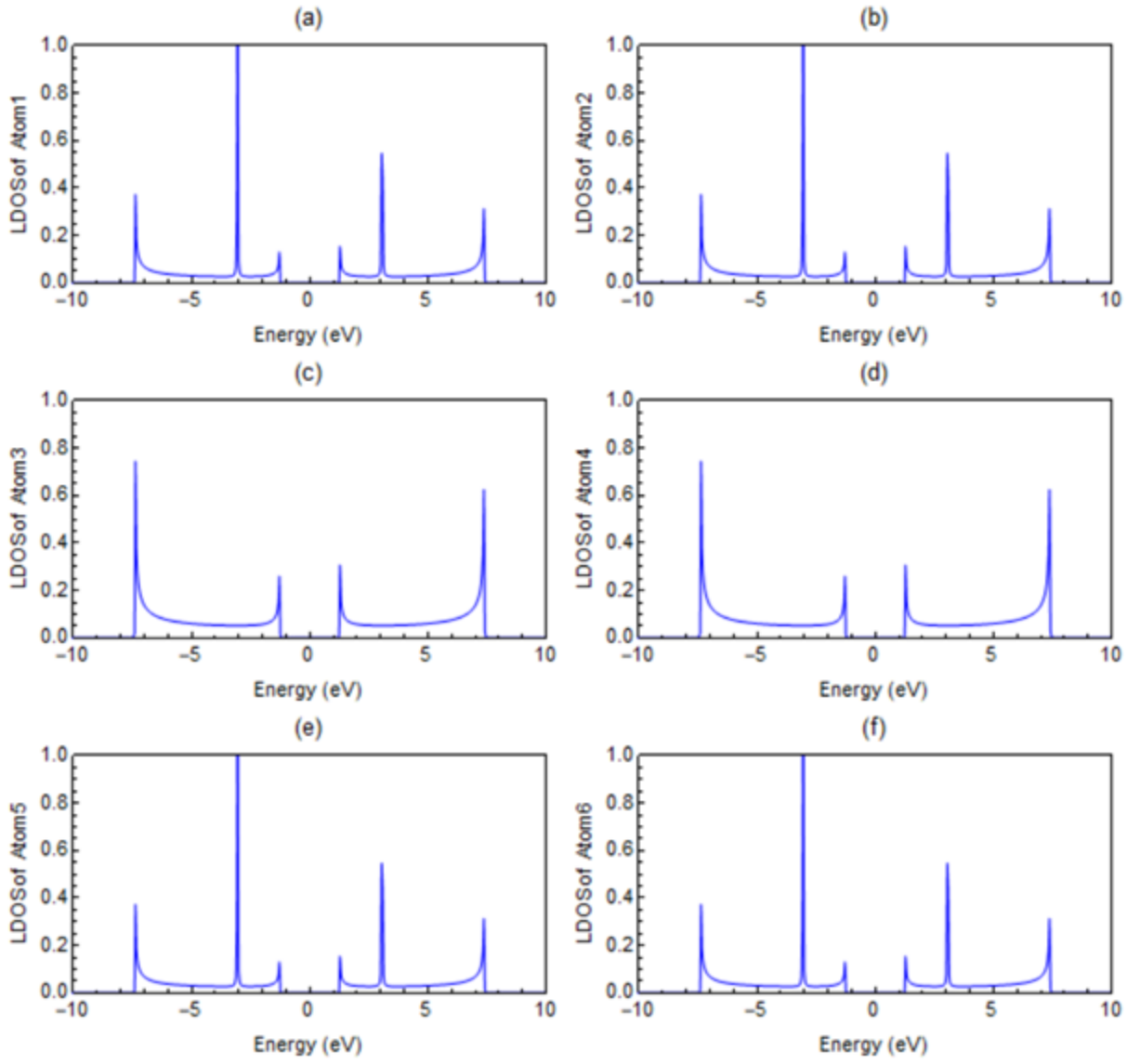

Figure 4.2: LDOS for pure n=3 AGNR using Hückel Theory.

Adding up all the individual LDOS produces the total DOS. LDOS values are lower than the DOS values because the values are only one part of the whole system. It is noticeable that the LDOS of atoms 1, 2, 5, and 6 are identical, and atoms 3 and 4 are also identical.

4.2.2 Conductance and LDOS for Pure n=3 AGNR Using Extended Hückel Theory

The conductance for the perfect AGNR using EHT is shown in Figure 4.3. There are more bands in the band structure and modes of transport in the conductance in the valence band region so it is not consistently at one multiple of the quantized value like with HT. This is due to the σ bonds, as observed in the characteristics of the electronic band structure which is shown in Figure 3.3 [5]. These small increases in conductance are exactly where extra, nearly flat bands occur in the band structure using EHT. Also, the material is a semiconductor. The band gap is again approximately 2.5 eV wide. Comparing the band structure from Chapter 3 and the conductance shows that the same number of bands are crossing as the amount of multiple integers of conductance is present at specific energies. For example, there are two bands crossing around - 4.6 eV in the band structure. One can see that in the conductance graph, the conductance rises up to the corresponding value of 2 ($\frac{2e^2}{h}$). There are no extra bands in the conduction band region of the band structure so that portion of the conductance stays the same as the HT result.

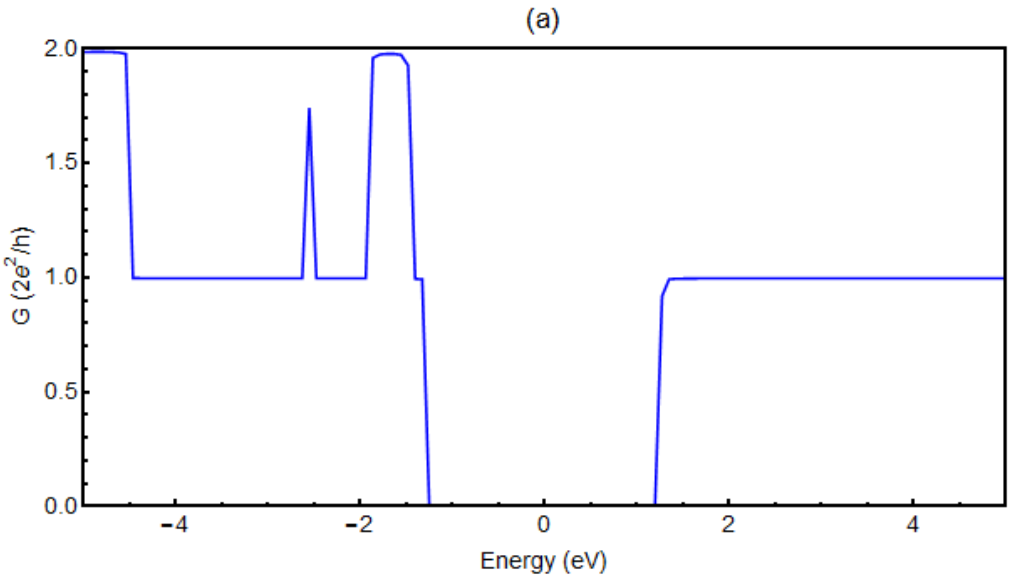

Figure 4.3: The conductance for pure n=3 AGNR using Extended Hückel Theory [5].

Edge termination is important because it cleans the conductance of rough areas, like what is seen in Figure 4.3. This is shown in the following section. At the edges of the pure structure, dangling bonds ruin the perfectly quantized behavior [5]. Like with HT, there are no modes of transport where the band gap is situated. Therefore, there is zero conductance. This is similarly seen in the DOS graph in Chapter 3.

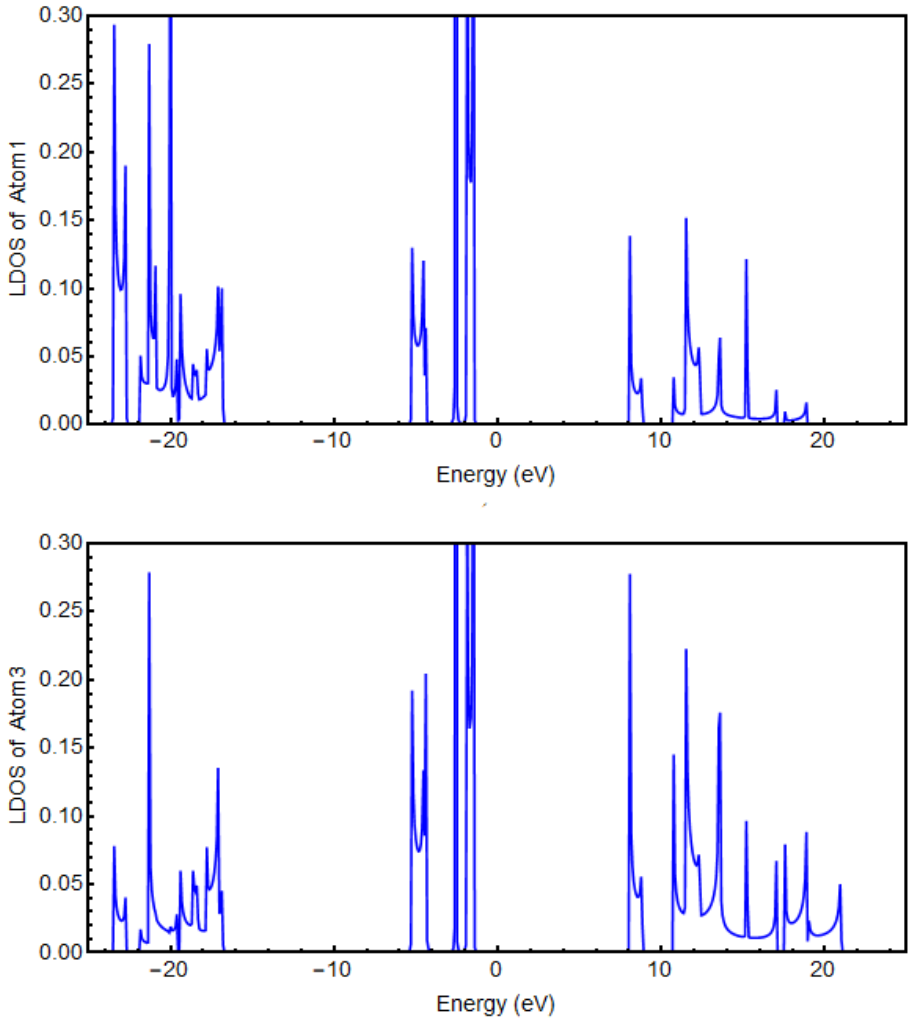

Figure 4.4: LDOS for pure n=3 AGNR using Extended Hückel Theory [5].

The LDOS for the perfect AGNR using EHT is shown in Figure 4.4. As seen with HT and EHT, there is symmetry. In other words, atoms 1, 2, 5, and 6 are identical and atoms 3 and 4 are similar too. In Figure 4.4, only the graphs for atoms 1 and 3 are shown because of this symmetry. Only the graphs for atoms 1 and 3 will be shown for the rest of the LDOS results. There are large peaks in the LDOS in Figure 4.4 wherever a flat band, also known as a stationary state, or a nearly flat band appears in the band structure shown in Chapter 3.

4.2.3 Conductance and LDOS for Functionalized n=3 AGNR: H, N, and O

This section will present the conductance and LDOS results for the n= 3 edge terminated AGNRs using EHT. The conductance and LDOS results will be shown as a direct comparison between the pure structure and the functionalized material. The functionalized results will be represented by the blue, solid line and the pure results will be represented by the dashed, orange line. The LDOS will only display atoms 1 and 3. As previously mentioned, this is because the LDOS for atoms 1, 2, 5, and 6 are identical and the LDOS for atoms 3 and 4 are identical.

Functionalized AGNR with H

The conductance for the AGNR functionalized with hydrogen using EHT is shown in Figure 4.5. The dashed line is the pure structure and the solid, blue line is the imperfect structure that is functionalized with hydrogen. As discussed previously, functionalizing the edges takes care of the dangling bonds and ultimately smooths out the conductance. The band structure from Chapter 3 only has one band crossing around $\pm$1.5 eV, which is reflected in how much conductance is shown in those areas in the graph. Interestingly, the conductance for H terminated AGNR using EHT is the same as the conductance for pure AGNR using HT. This is clearly shown in the band structure. The bands between approximately ±7 eV are the same in both the H terminated AGNR using EHT and the pure AGNR using HT band structure graphs. It is only past that range that the H terminated AGNR using EHT deviates. The transport near the Fermi

energy is mainly due to the pz orbitals. Therefore, it is expected. The band gaps show that the materials are semiconductors. After functionalization, the band gap does not change very much at all.

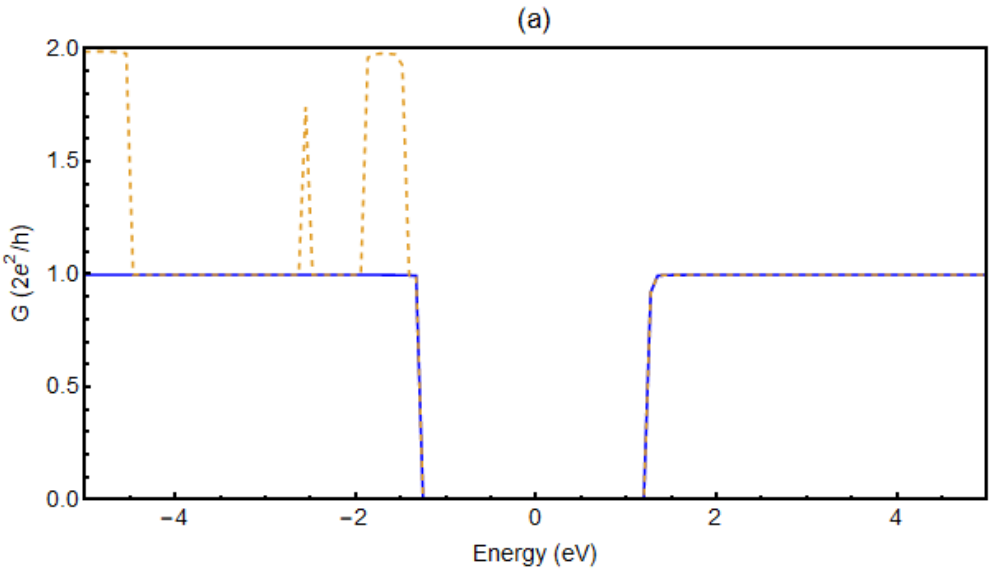

Figure 4.5: The conductance for a pure and functionalized with hydrogen n=3 dimer AGNR using Extended Hückel Theory. The orange, dashed line is the pure structure and the blue, solid line is for hydrogen.

Figure 4.6 displays the LDOS for the hydrogen terminated AGNR using EHT. The blue line is the hydrogen terminated results and the dashed, orange line is the pure results. The LDOS values for atom 1 is more negative than the LDOS of atom 3. As seen in Table 3.2, the onsite energy value for a hydrogen atom is more negative than the onsite energy for a carbon atom. The onsite energy and newly formed bonds are responsible for the changes. Also, the LDOS for atom 3

seems to be more positive. The LDOS for the pure structure has states near Fermi energy. When compared to the total DOS, the values are indeed smaller.

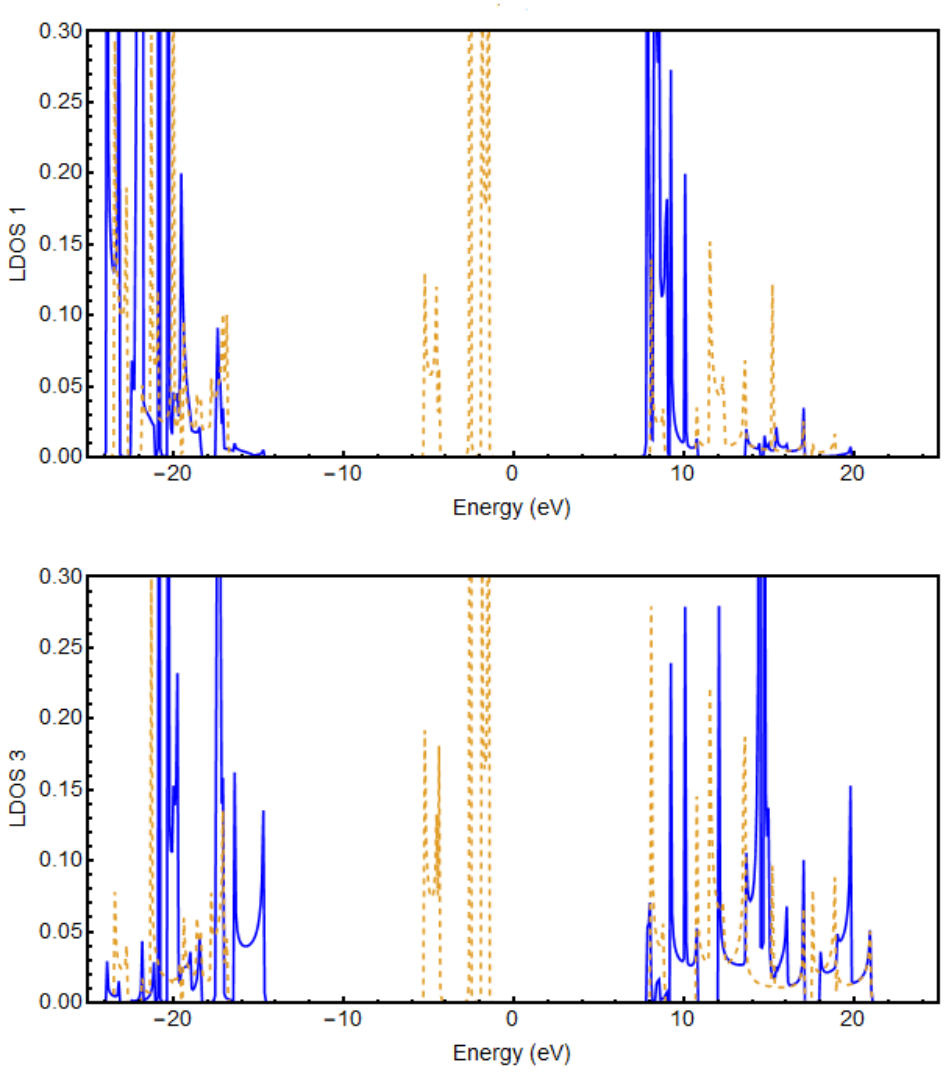

Figure 4.6: The LDOS for a pure and functionalized with hydrogen n=3 dimer AGNR using Extended Hückel Theory. The orange, dashed line is the pure structure and the blue, solid line is for hydrogen.

Functionalized AGNR with N

Figure 4.7 presents the results for the conductance of the AGNR terminated with nitrogen using EHT. The band gap shifts to the right after edge termination. In other words, the highest valence band is closer to the Fermi energy level and the lowest conduction band is farther from the Fermi energy level. The material is still a semiconductor, and the band gap decreases in size. After functionalization, the band gap is now around 2.2 eV. There are noticeably a lot more areas where the conductance drops to zero. This is also reflected in the band structure and the total DOS which are shown in Chapter 3.

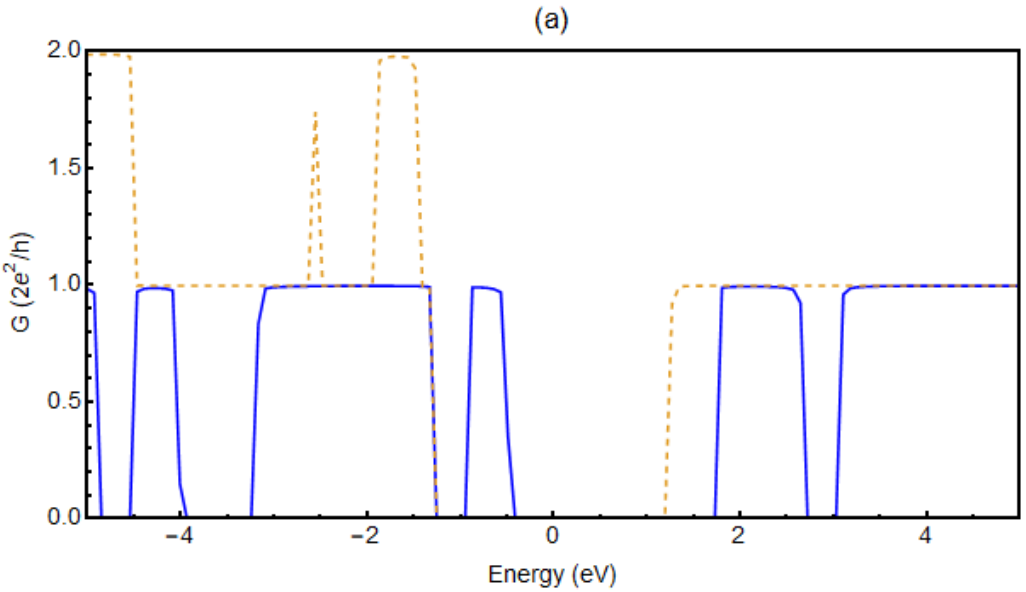

Figure 4.7: The conductance for a pure and functionalized with nitrogen n=3 dimer AGNR using Extended Hückel Theory. The orange, dashed line is the pure structure and the blue, solid line is for nitrogen.

Figure 4.8 shows the LDOS for AGNR terminated with nitrogen using EHT. The blue line represents the results for the N terminated AGNR and the orange line represents the results for the pure AGNR. Comparing the LDOS with the total DOS shows that the peaks are smaller in the LDOS. This makes sense because the LDOS is only one part of a whole. The LDOS for atom 3 has more positive states than negative states. Large peaks appear wherever a flat band occurs in the band structure.

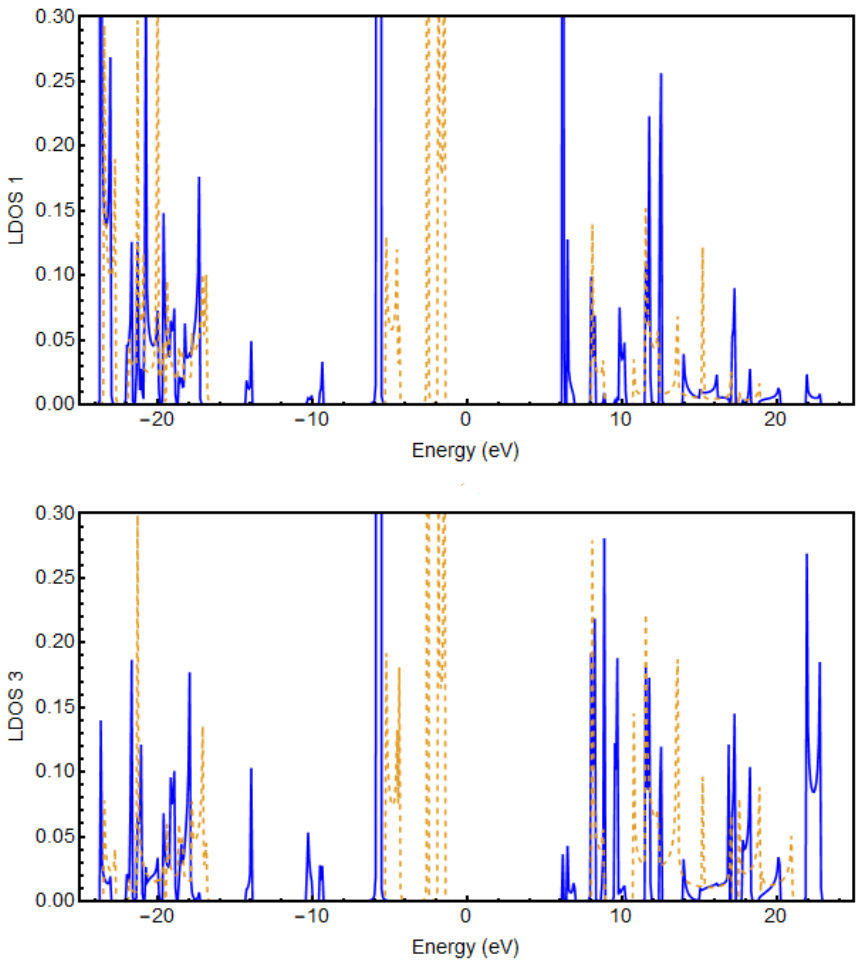

Figure 4.8: The LDOS for a pure and functionalized with nitrogen n=3 dimer AGNR using Extended Hückel Theory. The orange, dashed line is the pure structure and the blue, solid line is for nitrogen.

Functionalized AGNR with O

In Figure 4.9, the conductance for AGNR terminated with oxygen using EHT is displayed. There are more orbitals involved in this calculation so it makes sense to see a lot of

change between the pure structure and the functionalized structure, as seen with N edge termination. The band gap again shifts to the right toward the conduction band region. The material is still a semiconductor, and the band gap has decreased to around 2.2 eV. There are also noticeably more areas where the conductance drops down to zero. This is reflected in the band structure and DOS results in Chapter 3. In addition, there are a few energies where the conductance almost rises to an integer multiple of two for the conductance value. In the band structure in Chapter 3, there are no bands crossing around +3 eV and there is no conductance around that portion in the conductance graph.

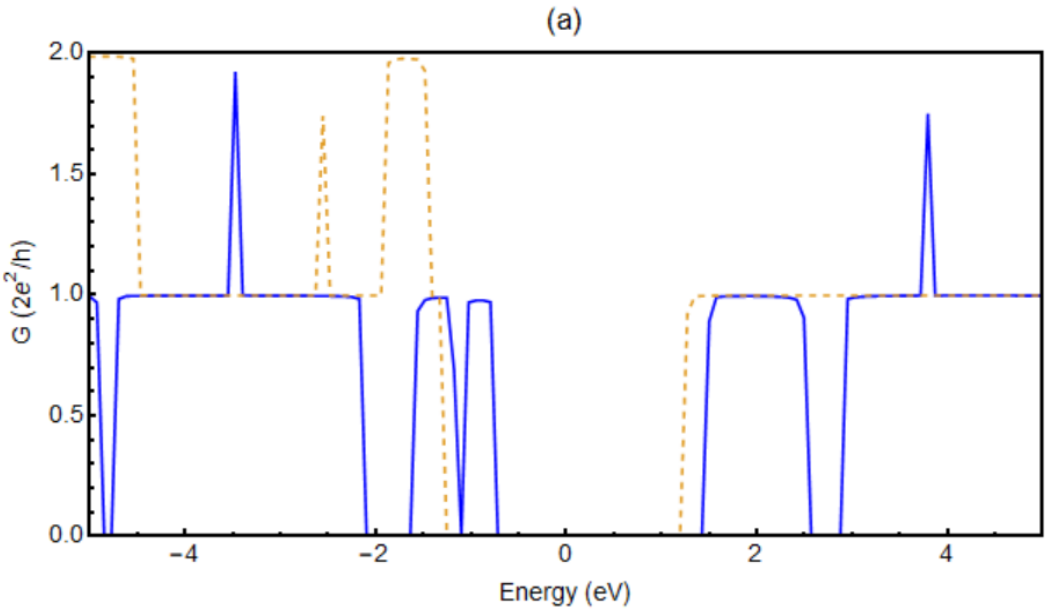

Figure 4.9: The conductance for a pure and functionalized with oxygen n=3 dimer AGNR using Extended Hückel Theory. The orange, dashed line is the pure structure and the blue, solid line is for oxygen.

Figure 4.10 presents the results for the LDOS of the AGNR terminated with oxygen using EHT. The blue line represents the O terminated AGNR LDOS, and the orange, dashed line represents the pure structure. Unlike the first two terminations where the LDOS for both the pure and the impure structures were relatively similar, the LDOS for the O functionalized AGNR seems more spread out than the pure structure. This is reflected in the band structure and total DOS shown in Chapter 3. The onsite energy of an oxygen is much more negative than the onsite energy of a carbon as shown in a table in Chapter 3.

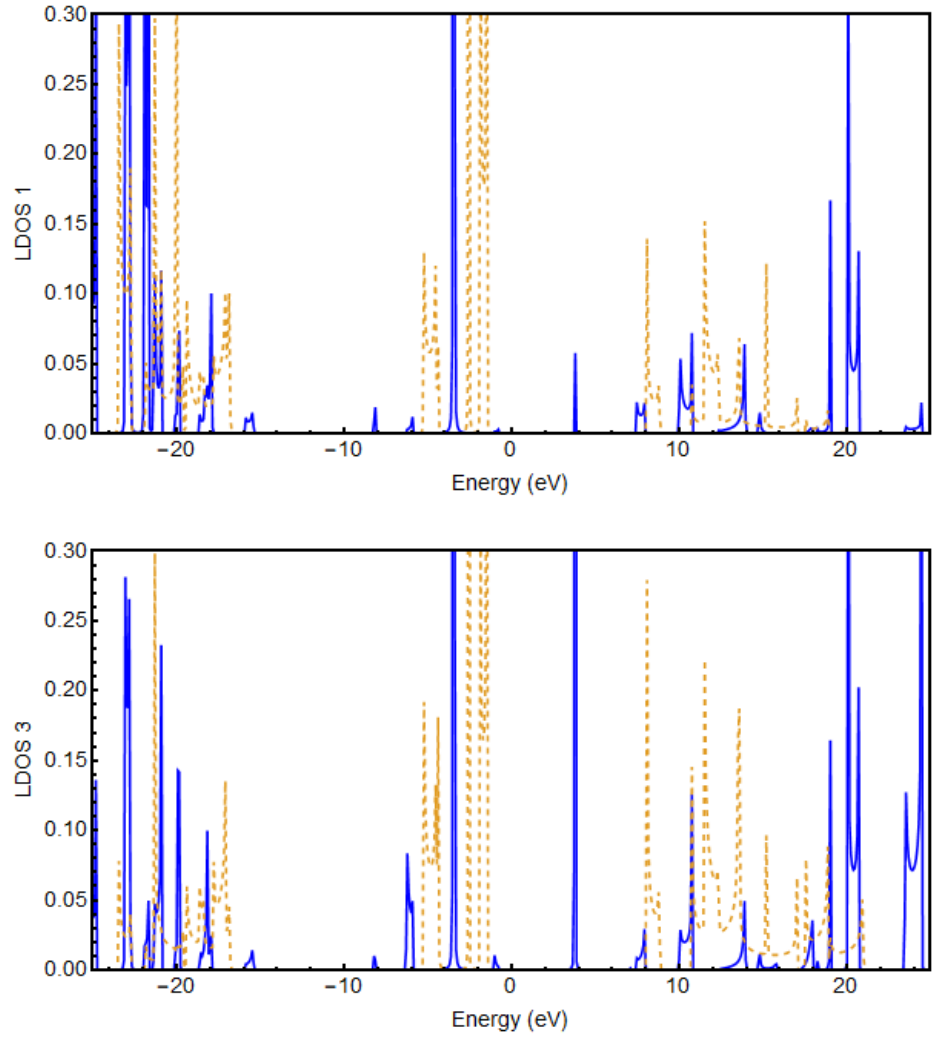

Figure 4.10: The LDOS for a pure and functionalized with oxygen n=3 dimer AGNR using Extended Hückel Theory. The orange, dashed line is the pure structure and the blue, solid line is for oxygen.

The conductance graphs show a change in the mode of electron transport. When functionalized, places where the conductance drops down to zero may appear that were not present in the pure structure. The band gap changes when the structure is functionalized with another element. The band gap may decrease slightly, and the band gap may even shift in one

direction. Higher integer multiples of conductance may appear too. This can similarly be seen in the LDOS.

4.3 Summary

This chapter presented the conductance and the LDOS results. First, the conductance and LDOS for pure AGNR using HT and EHT was discussed. Then, the conductance and LDOS results for AGNR functionalized with H, N, and O were presented. The LDOS for atoms 1, 2, 5, and 6 and the LDOS for atoms 3 and 4 are identical. Only the LDOS for atoms 1 and 3 were shown and only the H, N, and O edge terminated results were shown.

Conductance is essentially the modes of electron transport. Electron conduction relies on pz orbitals, as mentioned in an earlier chapter. LDOS shows the number states per energy for individual atoms. The number of states per energy is smaller for each atom in the LDOS because it is only one part of the whole system. Adding up all of the LDOS gives the total DOS and the number of states per energy is much higher than each individual part.

When functionalized, the modes of electron transport and the number of states per energy changed. Though, all of the structures that were shown are still semiconducting. This follows the dimer rule for odd values of n that n=3p, where p is an integer. The band gap did shift in one direction and the band gap slightly changed in size too in a few of the functionalized structures. After functionalization, the conductance had areas where it dropped down to zero due to a lack of crossing bands. Likewise, there are areas where the conductance increased.

Chapter 5: Summary and Conclusions

Chapter 1 served as an introduction to the thesis and the topic of interest. Graphene, discovered years ago, was found to be a very important material that has interesting electrical properties. Graphene is composed of carbons arranged in a repeating pattern of hexagons. Graphene nanoribbons (GNRs) are strips of graphene that are semi-infinite in one direction, and have a certain width. GNRs are also important, and can be used in various electronic devices. Band gaps can be tuned by various methods such as mechanical stress and introducing imperfection chemically and mechanically. Adding another element to the edges is one such method that changes the electrical properties. This research focused on the chemical method to alter the electronic properties of GNRs. GNRs can have zigzag or armchair edge structures. Two thirds of all armchair graphene nanoribbons (AGNRs) are semiconducting and one third are metallic. The classification depends on the width of the AGNR. Similarly, all zigzag graphene nanoribbons (ZGNRs) are metallic. AGNRs are described by dimers and ZGNRs are described by the number of chains in the structure.

Next, Chapter 2 discussed the theories used in the calculation in this thesis project. Carbon, the sixth element in the periodic table, has four electrons that can form bonds. There are four orbitals in carbon which are the s, px, py, and pz orbitals. These orbitals form π or σ bonds depending on which orbitals are forming bonds, and the direction the orbitals are facing. π bonds are weaker than σ bonds. The theories that were utilized in the calculations were: band structure, density of states (DOS), conductance, and local density of states (LDOS). The details on these theories have been presented in this chapter. The Tight Binding (TB) Model, the Hückel Theory (HT), and the Extended Hückel Theory (EHT) produce the band structure and density of states

(DOS). Only the nearest neighbor interactions were considered in the calculations. Only pz orbitals are utilized in the HT calculation, and all four orbitals are utilized in the more involved EHT calculation. The HT and the EHT are utilized in the TB Model. Using Schrödinger Equation (SE) and the total wavefunction, which is the linear combination of atomic orbitals (LCAO), the matrix elements of the Hamiltonian Matrix are obtained. The electronic band structure and DOS are obtained by solving the Hamiltonian Matrix.

Chapter 2 also discussed the Green's Function Theory and the Landauer Formula, which are used to calculate the conductance. In addition, Green's Function Theory produces the local density of states (LDOS). The structure is divided into three regions: the left lead, right lead, and the conductor. Conductance is the electron transport in a structure. Whereas LDOS is the density of states for an individual atom. The total DOS is the sum of all LDOS.

Chapter 3 focused on presenting functionalized AGNR using EHT. This chapter first showed the results for the band structure and DOS for n = 3 pure AGNR using HT and then the pure AGNR using EHT. These pure results were used to compare with the functionalized results. After the pure structures were displayed, the results for n=3 AGNR functionalized with H, N, O, F, P, S, and Cl using EHT were presented. Band structure is typically Energy vs. k and DOS is usually Energy vs. DOS. The DOS always reflects the band structure.

In Chapter 3, it was observed that pure AGNR using HT is symmetrical about Fermi energy, and has six bands. This pure structure is exhibiting semiconducting behavior. This structure follows the dimer rule. Next, the pure AGNR using EHT was found to not be symmetric about Fermi energy. Symmetry is due to the pz orbitals. The edge orbitals in the pure EHT calculation are not accounted for. Functionalization fixes this. It is observed on the pure AGNR using EHT band structure that the weaker π bonds are closer to Fermi energy, and the

bands at lower energies are from the stronger σ bonds. A flat band is a non-conducting band, otherwise known as a stationary state. The mass of an electron at a stationary state is very large, and the electron cannot move very well at all. Pure AGNR using EHT also exhibits semiconducting behavior.

Finally, in Chapter 3, the functionalized results utilizing EHT were displayed. When functionalized, the Hamiltonian matrix increases in size, and there are more orbitals and ultimately more bands in the band structure. Structures functionalized with H, N, O, F, P, S, and Cl are almost all found to be semiconducting, which follows the dimer rule, for odd values of n and where p is an integer, that n=3p. P edge functionalization exhibits more metallic behavior than semiconducting. When functionalized, more bands may appear in a section that was previously absent of bands in the perfect structure. More flat bands are observed than in the pure structure. There were a few structures where the band gap decreased in size. It was found that long bond length is related to a shorter band gap. Phosphorus and carbon have the longest bond length and the shortest band gap, and hydrogen and carbon have the shortest bond length and the longest band gap.

Chapter 4 displayed the local density of states (LDOS) and conductance results. First, the results for the conductance and LDOS of pure n=3 AGNR using HT and AGNR utilizing EHT were displayed. Then, the results for the conductance and LDOS of H, N, and O functionalized AGNR using EHT were then shown. The results were presented together with the pure results on the same graph for comparison between the features. All structures were shown to be exhibiting semiconductor behavior. The band gap either shifted in one direction, and/or changed in size slightly. When functionalized, areas where the conductance dropped down to zero appeared which were not present in the pure structure. The LDOS states per energy was smaller because it

is the DOS of a single atom. Adding all the LDOS together gives the total DOS that has a higher amount of states per energy. Only the LDOS for atoms 1 and 3 were displayed because the LDOS for atoms 1, 2, 5 and 6 are the same and the LDOS is the same for atoms 3 and 4.

References

1. S. Datta. *Quantum transport: atom to transistor.* Cambridge University Press. Cambridge. 2005.

2. Z. Kan. *Electrical properties of carbon structures: carbon nanotubes and graphene nanoribbons.* M.S. Thesis. Ball State University. 2013.

3. A. DiBenedetto. *The electronic properties of hexagonal boron nitride and graphene nanoribbon.* M.S. Thesis. Ball State University. 2017.

4. Z. Kan, C. Nelson, and M. Khatun. *Quantum conductance of zigzag graphene oxide nanoribbons.* J. Appl. Phys. 115 (15). 153704 (2014).

5. S. Jones. *Electronic properties of graphene nanostructure.* M.S. Thesis. Ball State University. 2016.

6. K. S. Novoselov, A. K. Geim, S. V. Morozov, D. Jiang, Y. Zhang, S. V. Dubonos, I. V. Grigorieva, and A. A. Firsov. *Electric field effect in atomically thin carbon films.* Science. 306. 666-9 (2004).

7. A. Lopez-Bezanilla, J. Huang, H. Terrones, and B. Sumpte, *Structure and electronic properties of edge-functionalized armchair boron nitride nanoribbons*. J. Phys. Chem. C. DOI: 116. 10.1021/jp3036583 (2012).

8. T. C. Li and S. Lu. *Quantum conductance of graphene nanoribbons with edge defects.* Phys. Rev. B. 77 (8). 085408 (2008).

9. N. Gorjizadeh and Y. Kawazoe. *Chemical functionalization of graphene nanoribbons*. Journal of Nanomaterials. 2010. (2010).

10. A. Simbeck, D. Gu, N. Kharche, P. Satyam, P. Avouris, and S. Nayak. *Electronic structure of oxygen-functionalized armchair graphene nanoribbons*. Phys. Rev. B. 88. 035413 (2013).

11. H. Zeng, J. Zhao, D. Xu, J. Wei, and H. Zhang. *Edge reconstruction limited electron transport of zigzag graphene nanoribbon*. Eur. Phys. J. B. 86 (2013).

12. H. Jippo and M. Ohfuchi. *First-principles study of edge-modified armchair graphene nanoribbons*. J. Appl. Phys. 113 (2013).

13. Y. Zhang, K. Zhou, K. Xie, J. Feng, H. Zhang, and Y. Peng. *Tuning the electronic structure and transport properties of graphene by noncovalent functionalization: effects of organic donor, acceptor and metal atoms*. Nanotechnology. 21. 065201 (2010).

14. F. Cervantes-Sodi, G. Csányi, S. Piscanec, and A. C. Ferrari, *Edge-functionalized and substitutionally doped graphene nanoribbons: Electronic and spin properties*. Phys. Rev. B. 77. 165427 (2008).

15. M. Stan, D. Unluer, A. Ghosh, and F. Tseng, *Graphene devices, interconnect and circuits - challenges and opportunities*. IEEE International Symposium on Circuits and Systems. 69-72. DOI: 10.1109/ISCAS.2009.5117687. (2009).

16. P. Shemella, Y. Zhang, M. Mailman, P.M. Ajayan, and S. Nayak. *Energy gaps in zero-dimensional graphene nanoribbons*. Appl. Phys. Lett. 91. 042101-042101. DOI: 10.1063/1.2761531 (2007).

17. E. Mucciolo, A.H. Castro Netro, and C. Lewenkopf. *Conductance quantization and transport gap in disordered graphene nanoribbons*. Phys. Rev. B. 79. 075407. 10.1103 (2009).

18. B. Wang, A. Baskin, and P. Král. *Porous nanocarbons: Molecular filtration and electronics*. Advances in Graphene Science. DOI: 10.5772/56247 (2013).

19. Z. Kan, M. Khatun, and A. Cancio. *Quantum transport in zigzag graphene nanoribbons in the presence of vacancies*. J. Appl. Phys. 125 (16). DOI: 10.1063/1.5079720 (2019)

20. P. Wagner, C. Ewels, J. Adjizian, L. Magaud, P. Pochet, S. Roche, and A. Lopez-Bezanilla. *Band gap engineering via edge-functionalization of graphene nanoribbons*. J. Phys. Chem. C. 117(50). 26790-6 (2013).

21. I. Martin and Y. Blanter. *Transport in disordered graphene nanoribbons*. Phys. Rev. B. 79. 235132 (2007).

22. Y.-C. Chen, D. Oteyza, Z. Pedramrazi, C. Chen, F.R. Fischer, and M.F. Crommie. *Tuning the band gap of graphene nanoribbons synthesized from molecular precursors*. ACS nano. **7**. DOI: 10.1021/nn401948e (2013).

23. O. Hod, J. Peralta, and G. Scuseria. *Edge effects in finite elongated graphene nanoribbons*. Phys. Rev. B. 76. 233401 (2007).

24. B. Xu, J. Yin, Y.D. Xia, X. Wan, K. Jiang, and Z.G. Liu. *Electronic and magnetic properties of zigzag graphene nanoribbon with one edge saturated*. Appl. Phys. Lett. 96. 163102. DOI: 10.1063/1.3402762 (2010).

25. S.-L. Chang, S.-Y. Lin, S.-K. Lin, C.-H. Lee, and M.-F. Lin. *Geometric and electronic properties of edge-decorated graphene nanoribbons*. Sci. Rep. 4. 6038. DOI: 10.1038/srep06038 (2014).

26. L. Brey and H. Fertig. *Electronic states of graphene nanoribbons studied with the Dirac equation*. Phys. Rev. B. 73. 235411 (2006).

27. V. Barone, O. Hod, and G. E Scuseria. *Electronic structure and stability of semiconducting graphene nanoribbons*. Nano letters. 6. 2748-54. doi: 10.1021/nl0617033 (2007).

28. L. Yang, C.-H. Park, Y.-W. Son, M. Cohen, and S. Louie. *Quasiparticle energies and band gaps in graphene nanoribbons*. Phys. Rev. Lett. 99. 186801 (2007).

29. A. Dibenedetto and M. Khatun. *Electronic properties of edge-terminated zigzag hexagonal boron nitride nanoribbons*. J. Phys. D: Appl. Phys. 52 (2018).

30. R. Saito and G. Dresselhaus. *Physical properties of carbon nanotubes*. London: Imperial College Press (1998).

31. Y. Zhang, J. Hu, X. Xie and W. Liu. *Abnormal electronic transport in disordered graphene nanoribbon.* Physical B-Condensed Matter. 404. 2259-2262 (2008).

32. W. Harrison. *Electronic structure and the properties of solids: the physics of the chemical bond.* Dover Publications, New York. 1989.

33. D. Griffiths. *Introduction to quantum mechanics, 2nd Ed.* Cambridge University Press. Cambridge. 2016.

34. A. Hinkle. *Tight-binding calculation of electronic properties of oligophenyl and oligoacene nanoribbons.* M.S. Thesis. Ball State University. 2008.

35. M. Buongiorno Nardelli. *Electronic transport in extended systems: application to carbon nanotubes*. Phys. Rev. B. 60. 7828 (1999).

36. A. Kimouche, M. Ervasti, R. Drost, S. Halonen, A. Harju, P. Joensuu, J. Sainio, and P. Liljeroth. *Ultra-narrow metallic armchair graphene nanoribbons*. Nat. Commun. 6:10177. DOI: 10.1038/ncomms10177 (2015).

37. M. Khatun, Z. Kan, A. Cancio, and C. Nelson. *Effects of band hybridization on electronic properties in tuning armchair graphene nanoribbon.* Canadian Journal of Physics. 94. 1-8 (2015).

38. H. Zheng, Z. Wang, T. Luo, Q. Shi, and J. Chen. *Analytical study of electronic structure in armchair graphene nanoribbons*. Phys. Rev. B. 75. 165414 (2007).

39. M. Ezawa. *Peculiar width dependence of the electronic properties of carbon nanoribbons.* Phys. Rev. B. 73. 045432 (2006).

40. Y. Miyamoto and K. Nakada. *First-principles study of edge states of H-terminated graphitic ribbons*. Phys. Rev. B. 59. 9858 (1999).

41. D.A. Areshkin, D. Gunlycke, and C.T. White. *Ballistic transport in graphene nanostrips in the presence of disorder: importance of edge effects*. Nano letters. 7. 204-10. DOI: 10.1021/nl062132h (2007).

42. M. Fujita, K. Wakabayashi, K. Nakada, and K. Kusakabe. *Peculiar localized state at zigzag graphite edge*. J. Phys. Soc. Jpn. 65. 1920. DOI: 10.1143/JPSJ.65.1920 (1996).

43. K. Nakada, M. Fujita, G. Dresselhaus, and M.S. Dresselhaus. *Edge state in graphene ribbons: Nanometer size effect and edge shape dependence*. Phys. Rev. B. 54. 17954-17961. DOI: 10.1103/PhysRevB.54.17954 (1997).

44. K. Wakabayashi. *Electronic properties of graphene nanoribbons*. NanoScience and Technology. 57. 277. DOI: 10.1007/978-3-642-22984-8_9 (2012).